

MULTI - SENSOR NAVIGATION SYSTEM DESIGN

DAVID ROYAL DOWNING



TRANSPORTATION SYSTEMS CENTER
55 BROADWAY CAMBRIDGE, MA 02142

MARCH 1971

TECHNICAL REPORT

AVAILABILITY IS UNLIMITED. DOCUMENT MAY BE RELEASED
TO THE NATIONAL TECHNICAL INFORMATION SERVICE,
SPRINGFIELD, VIRGINIA 22151, FOR SALE TO THE PUBLIC.

Prepared for
NATIONAL AERONAUTICS AND SPACE ADMINISTRATION
WASHINGTON, D. C. 20590

1. Report No.	2. Government Accession No.	3. Recipient's Catalog No.	
4. Title and Subtitle Multi-Sensor Navigation System Design*		5. Report Date March 1971	6. Performing Organization Code PG
7. Author(s) David Royal Downing		8. Performing Organization Report No. DOT-TSC-NASA-71-8	
9. Performing Organization Name and Address Transportation Systems Center Cambridge, MA 02142		10. Work Unit No. R1027	11. Contract or Grant No.
12. Sponsoring Agency Name and Address National Aeronautics and Space Administration		13. Type of Report and Period Covered Technical Report	
		14. Sponsoring Agency Code	
15. Supplementary Notes *Submitted in partial fulfillment of the requirements for the degree of Doctor of Science, at the Massachusetts Institute of Technology, May 1970.			
16. Abstract <p>This report treats the design of navigation systems that collect data from two or more on-board measurement subsystems and process this data in an on-board computer. Such systems are called Multi-Sensor Navigation Systems.</p> <p>The design begins with the definition of the design requirements and a list of n sensors and c computers. A Design Procedure is then developed which automatically performs a systematic evaluation of the $(2^n-1) \times c$ candidate systems that may be formed. This procedure makes use of a model of the navigation system that includes sensor measurement errors and geometry, sensor sampling limits, data processing constraints, relative computer loading, and environmental disturbances. The performance of the system is determined by its terminal navigation uncertainty and dollar cost. The Design Procedure consists of three design options, three levels of evaluation, and a set of auxiliary data. By choosing from among the design options and the auxiliary data, the designer can tailor the Design Procedure to his particular application.</p> <p>A design option is developed to answer each of the three following questions: (1) Which candidate system meets the system accuracy specification and has the lowest system cost? (2) For each sensor or computer chain, which is defined as the set of all systems containing that component, what is the system that satisfies the accuracy requirements and has the lowest cost? (3) Which systems satisfy the design accuracy requirements?</p> <p>The system evaluation is accomplished using one optimal and two non-optimal techniques. The optimal performance evaluation uses the measurement schedule that minimizes the terminal uncertainty. A first-order optimization procedure is developed to determine this schedule. This uses optimal sampling logic derived by applying the Maximum Principle. One non-optimal analysis uses the idea that the addition of a sensor or the increase of the computer processing capability can not degrade the system's performance. The second non-optimal technique obtains approximate values of the system's accuracy by assuming measurement schedules that do not satisfy the processing constraint.</p> <p>The Procedure is applicable to a large class of air or space missions for which a nominal trajectory can be defined. To illustrate how the Procedure would be used, the design of an aircraft navigation system for operation in the NE corridor is presented. This problem considers the configuration of a system starting with four candidate sensors and three candidate computers. The outputs from all three design options are presented and discussed.</p>			
17. Key Words .Multi-Sensor Navigation Systems .Design Procedure .Design Option .System Evaluation		18. Distribution Statement Unclassified - Unlimited	
19. Security Classif. (of this report) Unclassified	20. Security Classif. (of this page) Unclassified	21. No. of Pages 138	22. Price

CONTENTS

<u>Chapter</u>		<u>Page</u>
	SUMMARY	1
	SYMBOLS	3
	GENERAL NOTATION	5
1	INTRODUCTION	6
2	FUNCTIONAL DESCRIPTION OF MULTI-SENSOR SYSTEM DESIGN PROCEDURE	10
	2.1 INTRODUCTION	10
	2.2 FRAMEWORK OF DESIGN PROCESS	10
	2.3 ANALYTIC DESIGN PROCEDURE	12
3	FORMULATION OF THE DESIGN PROBLEM	16
	3.1 INTRODUCTION	16
	3.2 MODEL OF A NAVIGATION SYSTEM	16
	3.2.1 Mission Related Parameters	17
	3.2.2 System Related Parameters	18
	3.2.3 Mission Objective Parameters	22
	3.3 MATHEMATICAL FORMULATION	24
4	OPTIMAL SCHEDULING OF NAVIGATION MEASUREMENTS	28
	4.1 INTRODUCTION	28
	4.2 THEORETICAL DEVELOPMENT	28
	4.2.1 Continuous Measurement Formulation	28
	4.2.2 Necessary Conditions	30
	4.2.3 Formulation of Special Measurement Processes	37
	4.3 COMPUTATION ALGORITHM	39
	4.3.1 Algorithm Selection	39
	4.3.2 Computer Mechanization	41
	4.4 NUMERICAL EXAMPLE: OPTIMAL SCHEDULING OF DME MEASUREMENTS	46

CONTENTS (Continued)

<u>Appendix</u>		<u>Page</u>
A	THEORMS RELATING TO THE SWITCHING FUNCTIONS AND THE COVARIANCE PROPAGATION.	116
B	NAVIGATION IN A BENIGN ENVIRONMENT.	119
C	CHARACTERISTICS OF DIGITAL PROGRAM.	121
D	MODEL OF ENVIRONMENTAL DISTURBANCES	122
E	MEASUREMENT SENSITIVITY	126
F	PERFORMANCE INDEX SENSITIVITY FOR VARIATIONS IN CONTROL HISTORY	129
G	DESIGN PROCEDURE SYSTEM LISTING AND ANALYSIS SUMMARY	131
	REFERENCES.	136

MULTI-SENSOR NAVIGATION SYSTEM DESIGN

By David Royal Downing
Transportation Systems Center

SUMMARY

This report treats the design of navigation systems that collect data from two or more on-board measurement subsystems and process this data in an on-board computer. Such systems are called Multi-Sensor Navigation Systems.

The design begins with the definition of the design requirements and a list of n sensors and c computers. A Design Procedure is then developed which automatically performs a systematic evaluation of the $(2^n - 1) \times c$ candidate systems that may be formed. This procedure makes use of a model of the navigation system that includes sensor measurement errors and geometry, sensor sampling limits, data processing constraints, relative computer loading, and environmental disturbances. The performance of the system is determined by its terminal navigation uncertainty and dollar cost. The Design Procedure consists of three design options, three levels of evaluation, and a set of auxiliary data. By choosing from among the design options and the auxiliary data, the designer can tailor the Design Procedure to his particular application.

A design option is developed to answer each of the three following questions: (1) Which candidate system meets the system accuracy specification and has the lowest system cost? (2) For each sensor or computer chain, which is defined as the set of all systems containing that component, what is the system that satisfies the accuracy requirements and has the lowest cost? (3) Which systems satisfy the design accuracy requirements?

The system evaluation is accomplished using one optimal and two non-optimal techniques. The optimal performance evaluation uses the measurement schedule that minimizes the terminal uncertainty. A first-order optimization procedure is developed to determine this schedule. This uses optimal sampling logic derived by applying the Maximum Principle. One non-optimal analysis uses the idea that the addition of a sensor or the increase of the computer processing capability can not degrade the system's performance. The second non-optimal technique obtains approximate values of the system's accuracy by assuming measurement schedules that do not satisfy the processing constraint.

SYMBOLS

A	constant weighting matrix used in definition of System Performance Index.
CC	computer capacity (measurements/hour)
C1, C2, . . .	short hand designation of candidate computers
DT	time step used in numerical integration
DT_i	sampling interval for i^{th} sensor
\overline{DT}_i	minimum allowed DT_i
F	system linearized dynamics matrix
H	linearized measurement sensitivity matrix
\mathcal{H}	system Hamiltonian
\dot{i}	information rate
J	system performance index
J_{LC}	value of J computed using Limiting Case Analysis
J_{req}	value of J from system design specification
J^*	value of J computed using Optimal Measurement Schedule
K_i	Computer Loading factor for processing i^{th} sensor data (non-dimensional)
M/H	abbreviation for measurements/hour
N	measurement sample rate matrix (measurements/hour)
$N_i = N_{ii}$	sample rate for i^{th} sensor

GENERAL NOTATION

Vectors are indicated by a small underlined letter; matrices are designated capital letters.

Δ ()	incremental change in ().
δ ()	variational change in ().
() _{nom}	the variable () evaluated along the nominal trajectory
cov []	covariance matrix of [].

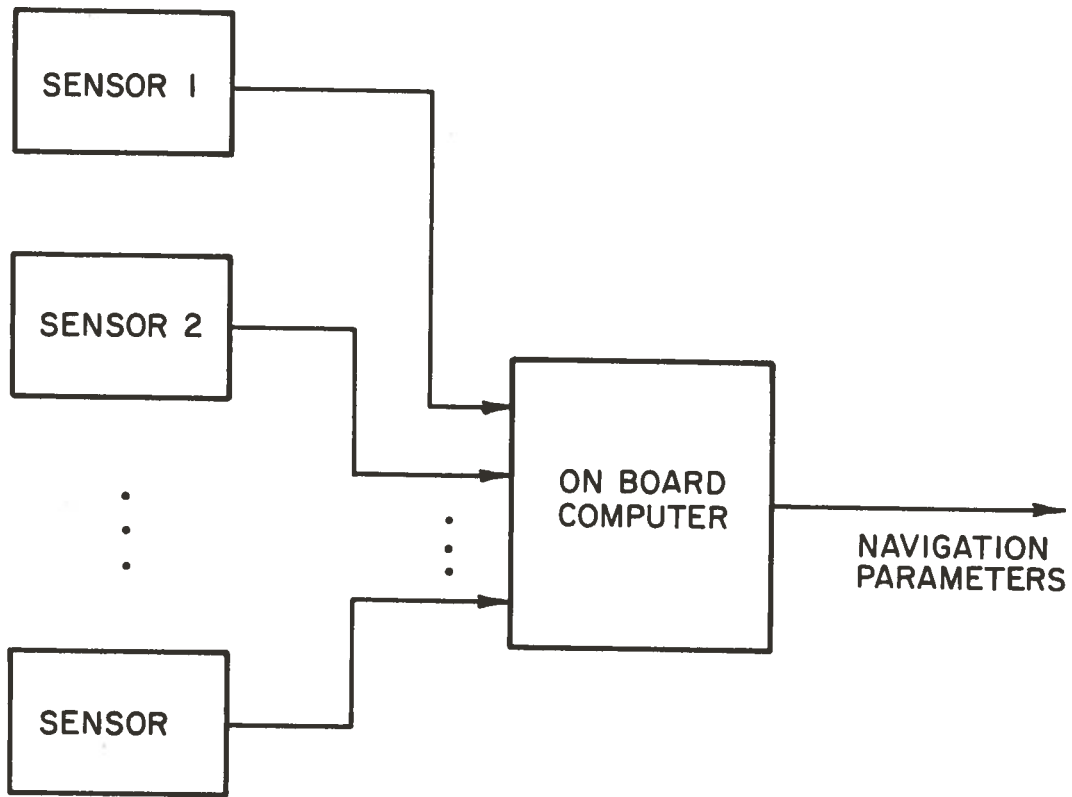


Figure 1.- Multi-sensor navigation system

tion allows the sensor sampling limitations and the processing limits to assume a convenient form. The technique then calls for a series of iterations on the sensor sampling rates to arrive at the optimal measurement schedule. To illustrate the optimization technique, the first example problem is presented. In this simple problem, the optimal measurement schedule is determined for a system which could measure range to two separate ground stations.

The Design Procedure is presented in Chapter 5. It consists of three design options, a set of selection logic for each option, three system evaluation techniques, and a set of auxiliary design data.

Each design option provides the designer with a different list of systems. The first option determines the Minimal System, i.e., the system that satisfies the design accuracy requirements and has the lowest total cost. Defining a component chain as a list of all systems that contain a given component, the second option determines the Minimal System for each sensor and computer chain. The third option determines all those candidate systems that satisfy the system accuracy requirements. The auxiliary data include the time histories of the estimation errors, the optimal measurement schedules and the corresponding sensor switching functions, and computer sensitivity data. By selecting from among the design options and auxiliary data, the designer can tailor the Design Procedure to his application.

The first evaluation technique makes use of the optimization procedure presented in Chapter 4. The second evaluation technique exercises the system using non-optimal measurement schedules that ignore the computer constraint to determine the system's limiting performance. The third technique uses the fact that a system's performance is never degraded if the system is augmented by additional sensors or computer capacity. Application of the two non-optimal evaluation techniques often allows candidate systems to be eliminated without the need of determining the optimal measurement schedule. To make efficient use of these three evaluation techniques, a different selection logic is generated for each of the design options. These sets of logic determine both the order in which the candidate systems are evaluated and also the order in which the evaluation techniques are applied to each system. An example problem is presented in Chapter 6 to demonstrate the Design Procedure. This design problem is the determination of the en-route navigation system to be used on a V/STOL aircraft for flights between Boston and Washington, D. C. Four candidate sensors and three candidate computers are considered.

Finally, Chapter 7 presents a summary of the present work and a discussion of several areas which are recommended for further study.

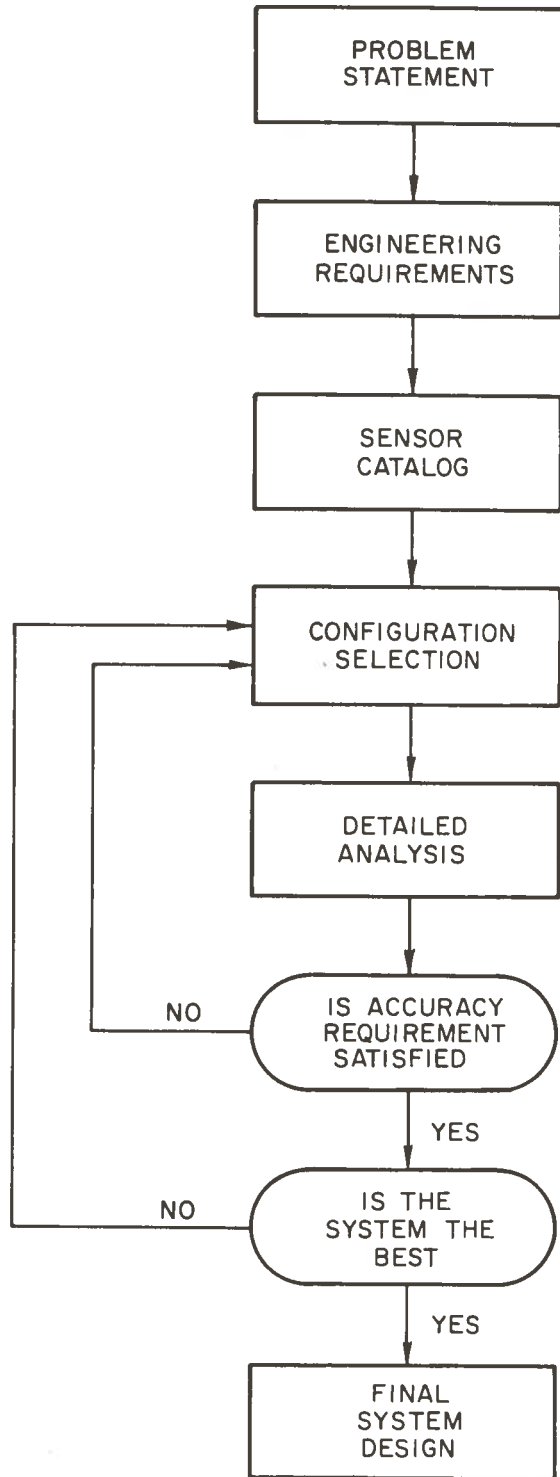


Figure 2.- Flow chart of design process

his past experience. The detailed analysis is performed on this subset and then the question is asked, "For the selected systems which is best and is this good enough?" This approach, although practical from a workload point of view, offers no assurance that a better configuration is not being overlooked. It is in the area between these two approaches that an analytic design procedure can be useful to the designer. The analytic design procedure provides additional data that fortifies and enhances the designers understanding of the design problem. With this additional information his selection of systems for detailed analysis can be made with greater confidence that the "best" system of the $(2^n-1)xc$ systems is not being overlooked.

Several general concepts can now be stated which will provide guidelines in the development of an automatic design procedure. First it will be required that the procedure determine the capabilities of all configurations by applying analysis at some level. This produces a high confidence in the selected configurations. If the design procedure is to save work, it is necessary that the level of analysis be less than used to perform the detailed analysis. Simplifications are made in both the definition of "best" and in the models used to evaluate the navigation systems. The factors which determine the relative ranking of systems include among other things system accuracy, cost, equipment availability, reliability, and maintainability. Instead of trying to model and weigh all these factors to form a super cost function, only the two considerations of system performance (in terms of accuracy) and system cost (in terms of dollars) will be used to evaluate configurations. Left to the designer is the tasks of applying the other factors at the time of selection of those systems on which further analysis will be performed. The second area of simplification is in the model of the navigation system. Such factors as sensor compensation, computation errors, and software mechanization are not considered. The models will, however, include the major influences on system performance, including sensor errors, computation limits, and environmental disturbances.

A second desirable feature for the design procedure is that it provides a variety of information allowing the designer choices which reflect his preference and the particular application. This feature is provided by identifying three design options and certain auxiliary information useful in the design and utilization of systems.

The total design process, including the design procedure, is shown in Figure 3. The functions of problem statement, conversion to physical terms, and the development of a catalog of candidate sensors and computers are tasks which are performed by the designer. The design procedure performs the tasks of configuration selection and evaluation.

The work remaining in the development of the design procedure are (1) the development of a mathematical model of a navigation system, and a specification of the design problem, (2) the development of a technique that allows the system's accuracy capabilities to be determined, and (3) a set of logic that allows the systematic analysis of all candidate configurations. The mathematical models of the navigation system and the design problem are given in Chapter 3. Chapter 4 presents the technique of determining the optimal schedule of navigation measurements used to evaluate systems. Chapter 5 presents the formulation of the design procedure including system evaluation and selection logic.

The definition of navigation presented in this work is the measurement and determination of the motion of the center of mass of the vehicle. It is possible to include the orientation vector as part of a larger navigation state vector \underline{x}' where:

$$\underline{x}' = \begin{bmatrix} \underline{x} \\ \underline{\phi} \end{bmatrix}$$

It is possible to separate the translational and rotational motions when configuring a navigation system, due to the fact that the vehicle's attitude control system has a higher bandwidth than the navigation system. It is assumed, therefore, that the vehicle's attitude will be held at its nominal value. Also, except for a few navigation sensors, e.g., inertial measuring unit, the rotational information is derived from a different set of sensors than those used to measure the motion of the center of mass.

From this starting point, it is possible to identify the important influences on the configuration of the navigation system. These factors are divided into mission related, system related, and mission objective related categories.

3.2.1 Mission Related Parameters

The parameters related to the mission are the vehicle, the trajectory, and the physical environment. Because only the function of navigation is of interest in this work, the vehicle can be modeled by its center of mass with its motion completely defined by Eq. (3.1).

For most applications, whether air, space, or marine navigation, the vehicle is constrained or controlled to be near a predetermined nominal trajectory. The nominal trajectory propagates according to the same dynamical equation as the vehicle model

$$\dot{\underline{x}}_{\text{nom}} = \underline{G}(\underline{x}_{\text{nom}}, \underline{\phi}_{\text{nom}}, \underline{U}_{\text{nom}}, \underline{W}_{\text{nom}}) \quad (3.3)$$

The final mission related factor affecting system design is the physical environment. The vehicle will travel through some physical environment during the mission; e.g., atmosphere, ocean, or space. The interaction of this environment with the vehicle will perturb the vehicle's motion. The effects of these environmental disturbances are of two basic types: (1) a deterministic component $\underline{W}_{\text{nom}}$ which can be included in the equation for the

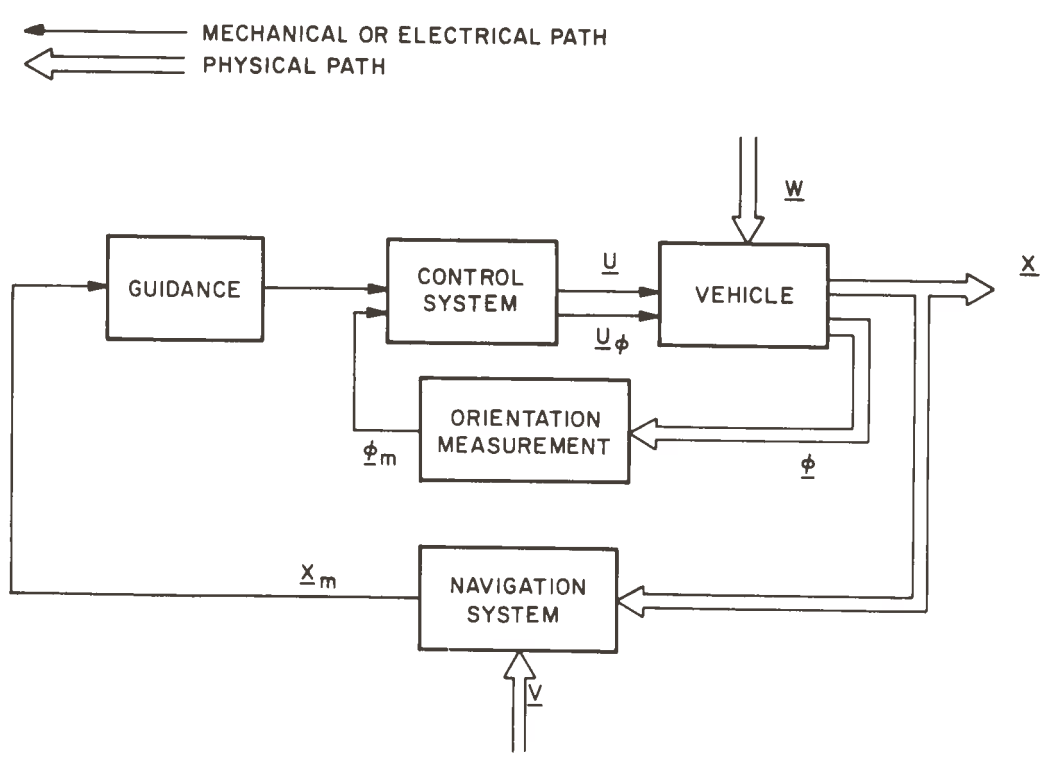


Figure 4.- Navigation, guidance, and control system

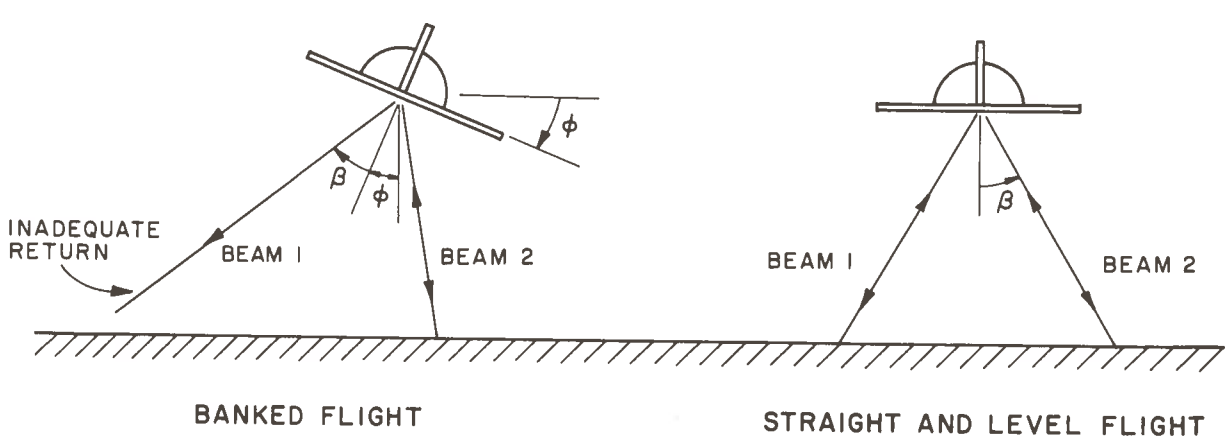


Figure 5.- Doppler radar geometry

Furthermore, a real sensor cannot make an exact measurement. There are two types of measurement errors. The first type is deterministic in nature and can be determined by preflight calibration. After calibration, it is possible to correct or compensate for these error sources. The second type of errors are those which are non-deterministic or random and by definition cannot be compensated. It will be assumed that the deterministic errors will be corrected and, therefore, will not be considered further.

The physical sources of the errors are of interest in developing realistic models. The information is, in general, corrupted by one or more of the following errors: receiver errors, information source errors, and errors associated with the propagation media. To account for these effects, sensor measurement accuracy is best modeled as the sum of a constant error plus an error dependent on the range to the source.

The final set of navigation sensor parameters are the maximum rates at which the sensors can be sampled. This limit can come from several physical sources; e.g., information is inherently in sampled form or if in continuous form, it must be sampled for use in the on-board digital computer. In any case there exists a set of constraints of the form:

$$DT_i \geq \hat{DT}_i \quad i = 1, \dots, m \quad (3.4)$$

where

DT_i = time between successive samples of the i -th measurement subsystem

\hat{DT}_i = smallest permitted time interval between successive samples of the i -th measurement subsystem

The measurements are processed in an onboard digital computer. The onboard computer is also responsible for performing the control and guidance computations and, therefore, only a certain portion of its total capacity will be assigned to the navigation computation. This assignment will be a percentage of the major cycle time of the computer. The amount of navigation data that can be processed in any given cycle is a function of two factors: (1) the amount of time assigned to navigation and, (2) the complexity of the required computations. The first factor is normally a design constraint, while the second factor is a design variable, i.e., the designer must make a trade-off of performance versus complexity of computation. To model relative computer requirements, a set of weighting factors must be derived which represent relative computer loading (relative to

$$\epsilon(t) = \hat{x} - x \quad (3.6)$$

The system accuracy is specified as a given function of the error in the estimate or the statistics associated with that error.

The second design objective is the minimization of system cost. Two distinct types of costs are associated with the navigation system's sensors and with the computer. The first is referred to as the Cost of Ownership and is modeled as a constant dollar cost. The Cost of Ownership includes such factors as initial purchase cost, maintenance costs, costs for special training of crews and maintenance personnel, required spare parts inventory, and ground equipment. Depending on the application, this cost may be amortized over many missions, as would be the case for a commercial airlines navigation system, or for only one flight for a launch vehicle application.

A second type of cost is one that is incurred during a mission and is a function of the use of the navigation system. An example of this kind of cost is the attitude fuel required to orient a spacecraft so that a navigation measurement can be taken. This cost is directly proportional to the number of measurements. In applications where both the cost of ownership and measurement costs are incurred, the cost function that is minimized when selecting the design has the form

$$J = (IC)_{\text{computer}} + \sum_{i=1}^m IC_i + \int_0^T \sum_{i=1}^m C_i N_i dt \quad (3.7)$$

where

IC_i = cost of ownership per flight for the i -th component

N_i = rate at which the i -th sensor is being sampled

C_i = weighting factors with units dollars/measurement

m = number of sensors

This cost function is minimized in a design where the accuracy requirement is a constraint on the design.

Virtually all applications have some form of Cost of Ownership. Not all have costs associated with measurement; e.g., an aircraft navigation system. For applications which have no Measurement Cost, the best system from a cost standpoint is that which meets the system performance requirements and has the lowest Cost of Ownership.

$$\sum_{i=1}^m K_i N_i \leq CC \quad (3.12)$$

The result of the processing is an estimate $\hat{\underline{X}}$ of the state vector

$$\hat{\underline{X}} = \hat{\underline{X}}(\underline{X}, \underline{Z}, t) \quad (3.13)$$

The system cost is the Cost of Ownership. Mission accuracy constraints are imposed only at the terminal time. The related problems which include Measurement costs and/or internal state constraints are discussed as recommendations in Chapter 7.

The first step in developing the mathematical framework is the use of the nominal trajectory to simplify the description of the problem. This simplification is accomplished by linearizing the state and measurement equations about the nominal trajectory. The linearized state equation is:

$$\dot{\underline{x}} = F(t)\underline{x} + G(t)\underline{\omega} \quad (3.14)$$

where:

$$F(t) = \left. \frac{\partial G}{\partial \underline{X}} \right|_{\text{nom}} + \left(\frac{\partial G}{\partial \underline{U}} \frac{\partial \underline{U}}{\partial \underline{x}} \right) \Big|_{\text{nom}}$$

$$G(t) = \left. \frac{\partial G}{\partial \underline{W}} \right|_{\text{nom}}$$

$$\underline{W} = \underline{W} - \underline{W}_{\text{nom}}$$

$$\phi = \phi_{\text{nom}}$$

Similarly a linearized form of the measurement vector is given:

$$\underline{z} = H_1(t)\underline{x} + H_2(t)\underline{v} \quad (3.15)$$

$$\underline{z} = \underline{Z} - \underline{Z}_{\text{nom}}$$

$$H_1(t) = \left. \frac{\partial Z}{\partial \underline{X}} \right|_{\text{nom}} ; H_2(t) = \left. \frac{\partial Z}{\partial \underline{V}} \right|_{\text{nom}}$$

$$\hat{x}_i^+ = \hat{x}_i^- + P_i^- H_i^T R^{-1} [z - H_i \hat{x}_i^-] \quad (3.20)$$

The covariance of the errors in the estimate propagates between measurements as:

$$P_i^- = \Phi_{i-1} P_{i-1}^+ \Phi_{i-1}^T + G_{i-1} Q_{i-1} G_{i-1}^T \quad (3.21)$$

with $P(t_0) = P_0$

and $P(t)$ is changed after a measurement as:

$$P_i^+ = P_i^- - P_i^- H_i^T (H_i P_i^- H_i^T + R_i)^{-1} H_i P_i^- \quad (3.22)$$

A few words are in order at this point concerning the model assumed for the measurement errors and the system disturbances. Although White Noise does not exist in the physical world, the use of it in the mathematics does not introduce significant errors. The applications where this is true are those that have broad-band noise acting through a dynamic system. If the bandwidth of the noise is larger than the bandwidth of the system, then using White Noise models of the noise is an accurate assumption. For applications where this relation between the system and noise bandwidths does not exist, techniques exist (ref. 4) which give an estimation error propagation of the same form as Eqs. (3.21 and 3.22). These techniques use shaping filters to process the White Noise and then they expand the state vector by the inclusion of the correlated noise variables. This then is a system which has a larger state but is then considered to be driven with white noise.

The elements of the covariance matrix of the estimate errors are functions of the nominal trajectory, measurement errors statistics, measurement sequence, system disturbance statistics, and measurement geometry. For a configured system and a prescribed mission, the only one of these parameters available to the designer is the sequence of navigation measurements. There exists a particular history of navigation measurements that gives the minimum value of the accuracy measure $A(P(t))$. To determine this optimal measurement schedule requires the solution of an optimal control problem. A statement of this problem is, "Find the sequence of measurements, subject to the sampling and processing constraints (Eqs. 3.12, 3.13), such that the value of $A(P(t))$ is minimized where $P(t)$ propagates according to (Eqs. 3.22 and 3.23)." In the next chapter, an iterative optimization procedure is developed which determines the optimal schedules.

due to the form of the constraints. To alleviate this difficulty, the discrete measurement process is reformulated as a continuous measurement process. It can be argued (ref. 5) that if the interval between discrete measurements is small compared to system characteristic times and if the change in system measurement geometry is small, then the sequence of discrete measurements, with mean squared measurement error σ^2 , can be approximated by a continuous measurement process with

$$\text{cov } [v] = \sigma^2 DT \delta(t - \tau) \quad (4.1)$$

For the estimation of a continuous state using continuous measurements, the estimation error covariance matrix $P(t)$ can be shown (ref. 6) to satisfy

$$\dot{P} = FP + PF^T - PH^TNR^{-1}HP + Q \quad (4.2)$$

where

$$N_{ij} = \begin{cases} \frac{1}{DT_i} & i = j \\ 0 & i \neq j \end{cases}$$

and

$$R_{ij} = \begin{cases} \sigma_i^2 & i = j \\ 0 & i \neq j \end{cases}$$

The control variables are the elements of N_i each of which is the rate at which its corresponding sensor i is sampled. Also, the measurement constraints given by Eqs. (3.12) and (3.13) take the natural form:

$$N_{ii} \leq NM_i \quad i = 1, \dots, m \quad (4.3)$$

Finally writing the term involving N in series form

$$\mathcal{H} = \sum_{i=1}^m (-R^{-1}HPAPH^T)_{ii} N_{ii} + \text{tr}\Lambda(FP + PF^T + Q) \quad (4.7)$$

An examination of the Hamiltonian and the inequality constraints shows that all three are linear in the control variables. This indicates that this problem is a linear optimization problem and the necessary conditions for optimality can be determined by applying Pontryagin's Maximum Principle (ref. 7). For the problem defined by Eqs. (4.2), (4.3), (4.4), (4.5), and (4.7), the Maximum Principle states; as follows.

If the costate matrix satisfies:

$$\begin{aligned} \dot{\Lambda} &= -\Lambda F - F^T \Lambda + H^T N R^{-1} H P \Lambda + \Lambda P H^T N R^{-1} H \\ \Lambda(T) &= A \end{aligned} \quad (4.8)$$

then the optimal N(t) is that value of N(t) which satisfies the control constraints (Eqs. (4.3) and (4.4)) and minimizes the system Hamiltonian for all $0 \leq t \leq T$.

To see what form the control takes, consider first the case without the computer constraint. Upon examination of the Hamiltonian, it can be seen that the controls which minimize Eq. (4.7) are given by:

$$(N_{\text{OPT}})_{ii} = \begin{cases} 0 & , \quad SW_{ii} > 0 \\ NM_{ii} & , \quad SW_{ii} < 0 \end{cases} \quad (4.9)$$

where SW_{ii} are known as the switching functions and are given by:

$$SW_{ii} = -(R^{-1}HPAPH^T)_{ii} \quad (4.10)$$

The logic defined by Eqs. (4.3) and (4.4) defines the admissible control region which for m measurements is an m dimensional hypercube. The case $m = 2$, is shown in Figure 8. The control defined by Eq. (4.9) is known as Bang-Bang control because it is

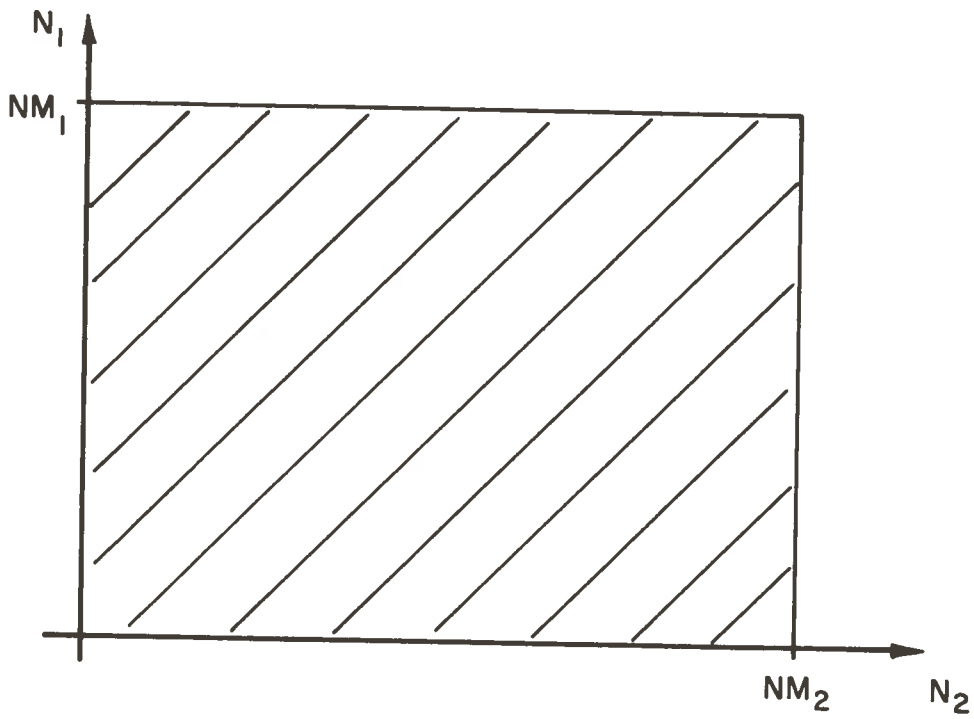
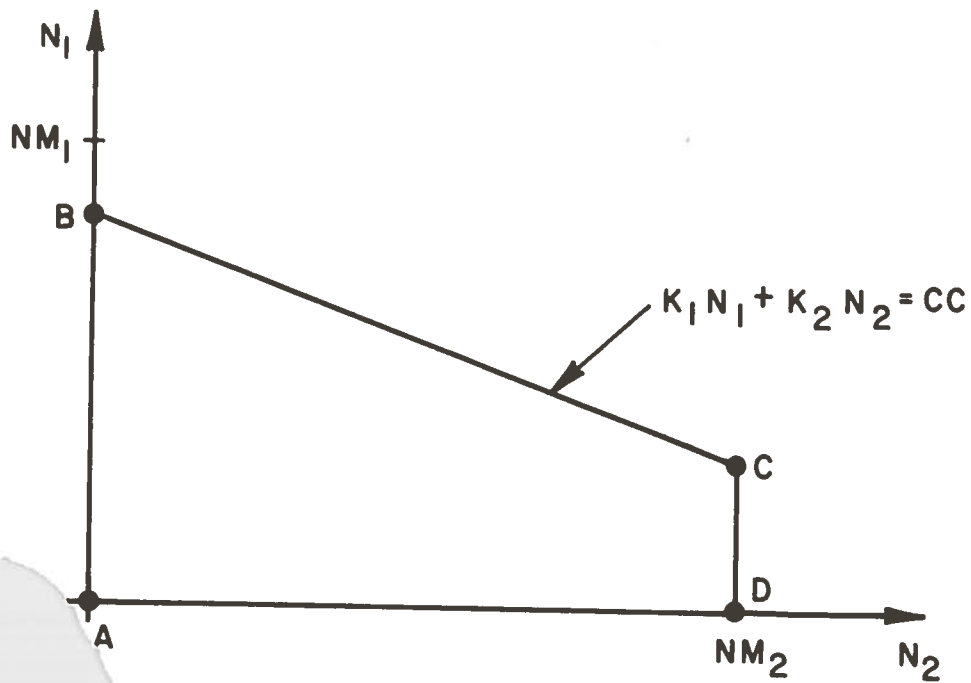


Figure 8.- Admissible control region with magnitude limiting



9.- Admissible control region with magnitude and computer limiting

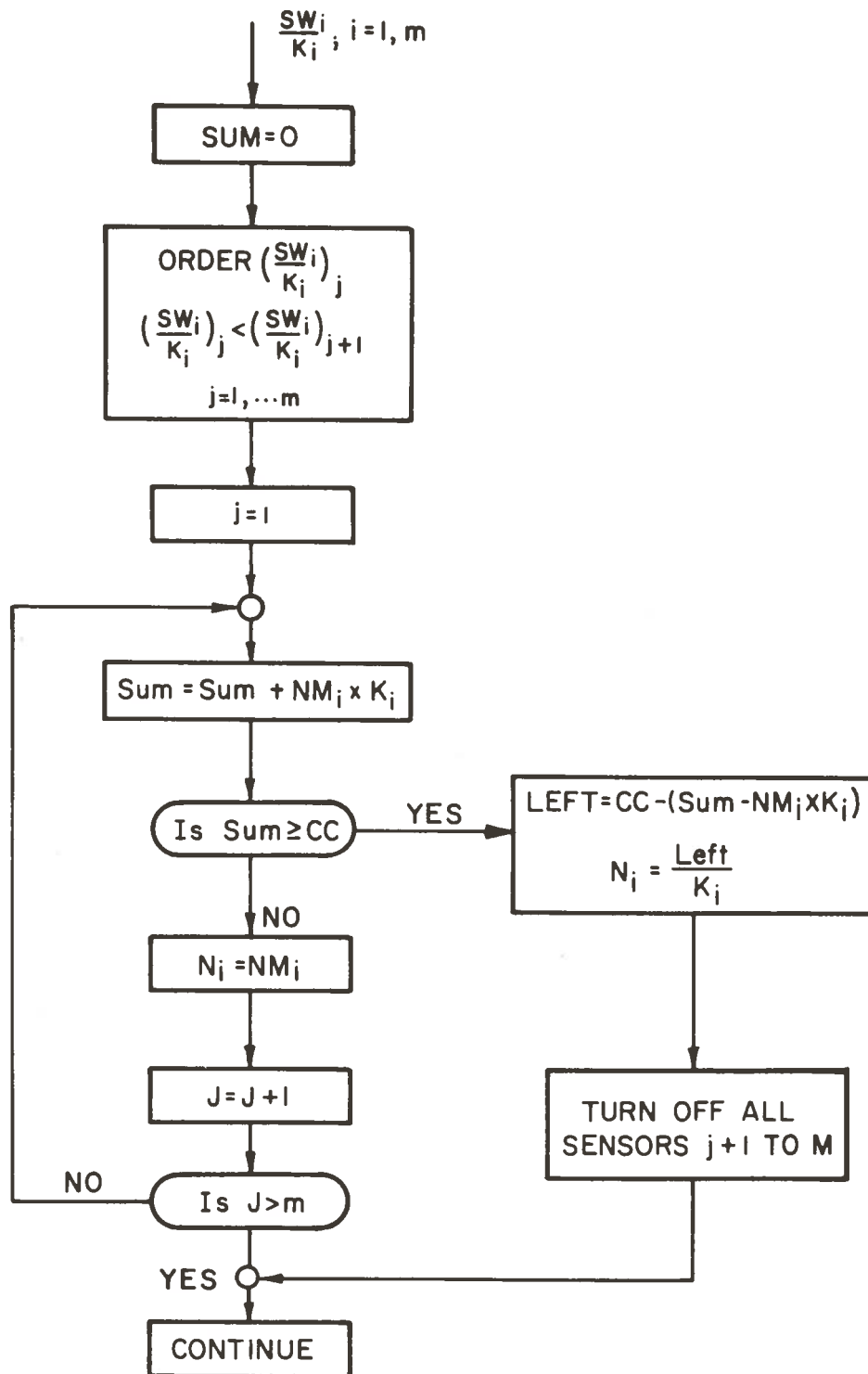


Figure 10.- Computer constrained optimal control strategy

4.2.3 Formulation of Special Measurement Processes

Thus far, the formulation of the measurement scheduling problem has been in terms of m independent sensors. Each sensor has associated with it a scalar measurement with measurement error R_{ij} . This measurement is related to the state variable through the $1 \times n$ geometry matrix H_i . In the modelling of the navigation sensors of Section 3.2.2, two types of sensors which do not directly fit into the above description were identified. These two cases are the multi-source sensors and the multi-measurement sensors. In both cases a slight modification to the optimal switching criteria must be developed. This development follows.

Multi-Source Sensors.- There exists a group of sensors which are capable of deriving information from several external sources. An example of this type of sensor is a Distance Measuring Equipment (DME) (used by aircraft). The DME measures the range from the sensor to known ground stations. Referring to Figure 11, it can be seen that the geometry and measurement accuracy which are modeled as functions of range depends on the source being sampled. Another characteristic of this type of Multi-Source Sensor is that only one source can be sampled at any time. This limitation is due to the fact that each ground station operates at a different frequency as a means of identification. A similar limitation is true for the class of startrackers that can track only one star at a time, e.g., a Canopus tracker. With this class of sensor, the switching matrix must be partitioned and an additional logic step included. First, associated with each source is its geometry and measurement error covariance. The switching matrix will be $M \times M$, where M is the total number of measureables, i.e., the number of sources of information. Those diagonal elements corresponding to a particular sensor are collected and the source whose information is most efficient is identified. This weighted switching function will then be the one used for that sensor in the logic given in Figure 10.

Multi-Measurement Sensors.- Another class of sensors which requires special consideration is that in which the sensors simultaneously measure several independent scalar quantities. An example of such a sensor is a doppler radar used on aircraft. As shown in Figure 12, there are four radar beams which are sampled simultaneously. It does not take significantly more computation to process the information from four beams than from one beam and, therefore, it does not make sense to disregard the information from any of the beams. Each beam has a different geometry matrix $H_i(t)$ and, therefore, each beam will have a switching function. The total efficiency of the doppler radar is the sum of the corresponding switching functions. The switching function used in the optimal control logic Figure 10 is:

$$\left(\frac{SW}{K}\right)_{\text{Doppler}} = \frac{SW_{\text{Beam 1}} + \dots + SW_{\text{Beam 4}}}{K_{\text{Doppler}}} \quad (4.13)$$

4.3 COMPUTATION ALGORITHM

The development of an algorithm to solve the optimization of the measurement schedule involves the determination of which necessary conditions are to be satisfied on any iteration and which conditions are to be iterated. Having made this selection, it is necessary to determine the scheme that will be used to mechanize these equations on a digital computer. This involves the selection of numerical integration schemes, time step and iteration controls. A brief description of the computer program and the digital machine on which it was used is given in Appendix C.

4.3.1 Algorithm Selection

An optimization procedure based only on first-order information was selected for this problem. This procedure was found to converge in a reasonable number of iterations and avoided the complexities that would have resulted from the large number of Bang-Bang controls in a higher order scheme. The particular optimization technique employed was the procedure known as the "Approximation to the Solution" (ref. 7). The procedure is not a simple gradient method; in fact, gradient information is never calculated. Rather this procedure, shown in Figure 13, performs an iteration on the control history by integrating the state equation:

$$\dot{P} = FP + PF^T - PH^TNR^{-1}HP + Q \quad (4.14)$$

from $t = 0$ to $t = T$, using the known initial condition P_0 , terminal time T and an assumed control history $\bar{N}(t)$. The values of $P(t)$ are stored during the forward integration and used to integrate the costate equations:

$$\dot{Z} = (F + P^{-1}Q)Z + Z(F^T + QP^{-1}) \quad (4.15)$$

backward from $t = T$ to $t = 0$, starting with $Z(t) = P(t)\Lambda(t)P(t)$. At each point in the backward integration, the optimal control logic given in Figure 10 is applied to determine the control $N^*(t)$.

Since $N^*(t)$ is based upon a $P(t)$ derived from $\bar{N}(t)$, the two control histories will not agree. The error is then used to update $\bar{N}(t)$ for the next iteration.

The advantage of this procedure is that both the state and the costate equations are integrated in their stable direction from known boundary conditions. This eliminates the problems associated with the numerical integration of an unstable equation. The main disadvantage is the requirement that $P(t)$ be stored at each time step in the forward integration. The storage required for an n dimensional state with N_{DT} integration steps is $1/2 n(n + 1) N_{DT}$ which can be substantial for large dimensioned state equations.

4.3.2 Computer Mechanization

The optimization procedure shown in Figure 13 has three parts; the integration of the state and costate equations, the application of the optimal switching logic, and the generation of the increment in the control variables. The mechanization of the optimal switching logic follows from straight forward programming of Figure 10, and will not be discussed here.

Integration Scheme.- To integrate the state equation forward in time, a fourth-order Runge-Kutta integration scheme was selected. For the backward integration of the costate equation, a second-order Runge-Kutta scheme was used. These schemes (refer to Table I) were selected because of their simplicity and accuracy.* The use of a Second-Order Runge-Kutta Scheme for the backward integration is compatible with the forward integration scheme in that the required values of $P(t)$ at the beginning and end of each time step are available. Unlike some other schemes that numerically integrate differential equations, as for example in the predictor corrector class of integration schemes (ref. 8), Runge-Kutta techniques do not have a built-in variable time step control. Such control is required because the covariance equations can have several time intervals where large derivations occur. These intervals depend on the control history and will shift when changes in control are made. A time step control was developed which controls the error between a predicted value of the $P(t)$ and the value generated by the fourth-order Runge-Kutta integration by adjusting the time step. This procedure starts with the value of the derivative \dot{P}_{i-1} at time t_{i-1} , and the time step DT_i as shown in Figure 14. Using the value of $P(t_i)$ and

*The error in the fourth order is proportional to $(DT)^5$ and the second order to $(DT)^3$ (ref. 8).

Eq. (4.14), the derivative $\dot{P}(t_i)$ is calculated. For a guess at DT_{i+1} , say \overline{DT} , a linearly predicted value of $\dot{P}(t_{i+1})$, $\overline{\dot{P}}(t_{i+1})$ is calculated. Using $\overline{P}(t_i)$, $\overline{\dot{P}}(t_i)$, and $P(t_{i+1})$, calculate:

$$\overline{P}(t_{i+1}) = P(t_i) + (\dot{P}_i + \overline{\dot{P}}_{i+1}) \frac{DT_{i+1}}{2} \quad (4.16)$$

Using \overline{DT} and the corresponding values of P_i and t_i the fourth-order algorithm computes $P(t_{i+1})$. If the values of $P(t_{i+1})$ and $\overline{P}(t_{i+1})$ agree to within a prescribed accuracy ϵ_1 the step is accepted. If the error is too large, the time step \overline{DT} is halved and the process repeated. This procedure is the first loop shown in Figure 15. It can be seen that if \overline{DT} is much too large, several cycles are required and a large amount of computer time is required. Also, after a region in which very small time steps are required is passed, it would be inefficient to retain this small value of DT . The second loop in Figure 15 indicates the logic used to increase the time step. Again, the error in the prediction is used as the guide to the time step. Two limits are introduced, ϵ_2 and $(DT)_{\max}$. If the error is less than ϵ_1 but greater than ϵ_2 the latest acceptable time step is again tried. If the error is less than ϵ_2 , the time step is doubled for the next pass. Finally, since the time step history cannot be generated solely on the behavior of the forward integration (these same time steps are used in the backward integration) a limit is put on the maximum value of DT . A satisfactory set of limits ϵ_1 , ϵ_2 , and DT_{\max} depend on the application and may require some experimentation.

Control Iteration.- To perform the forward integration of the covariance equation, it is necessary to assume a control history $\overline{N}(t)$. Once having $P(t)$ it is possible to perform the backward integration of $Z(t)$ and, by applying the logic given in Figure 11, to calculate the control history $N^*(t)$. The minimum cost is the cost corresponding to the situation where $\overline{N}(t) = N^*(t)$.

To arrive at this condition a procedure must be developed which uses the error quantity $\overline{N} - N^*$ to develop an increment in control $\delta N(t)$. Then, letting $\overline{N}(i) = \overline{N}(i-1) + \delta N(i)$, the procedure is repeated until the error is reduced to an acceptable level.

Because of the bang-bang nature of the control functions, care must be taken in developing a procedure for determining $\delta N(t)$. This is required so that the N^* is well behaved. The procedure developed in this work is a modification of Jacobson's first order Differential Dynamic Programming technique (ref. 9).

It is characterized by the fact that only a portion of the control history is interpolated on each pass. Although apparently this type of iteration requires more passes through the equations than a scheme which interpolates between the full \bar{N} and N^* histories, this is not true in general. The reason is that interpolation can cause large δP and $\delta \Lambda$ and thus produce N^* which are less representative of the true optimal.

To illustrate the procedure, consider the set of forward and backward control histories given in Figure 16. These controls correspond to a contrived situation in that for the system with one sensor there are three measurement rates 60, 30 and 0 M/H. This situation could never exist, since by the logic given previously, a single sensor can only have one level whose value is either on the computer constraint or the sampling constraint boundary. It is convenient, however, to use only a single control variable to develop the control iteration scheme. Also for convenience the control histories are converted into tabular form. This form includes a number and time for each switch in a control; i.e., each time a control variable changes magnitude. Also associated with each switch is the value of all controls just prior to the switch. The tabular representation of the control histories shown in Figure 16 is listed in Table II, starting with switch 1, the values of \bar{N} and N^* are compared. If they are equal (as in the case) switch 2 is considered. The case where \bar{N} and N^* are not equal will be considered shortly. At switch 2, the controls \bar{N} and N^* just to the left of the switches are again equal and, therefore, the Number 2 switches differ only in the time at which the switches occur. As an increment in the next assumed control, the second switch point is updated using the algorithm

$$t_2^{(1)} = t_2^{(0)} + \epsilon_4 \left(t_2^{*(0)} - t_2^{(0)} \right) \quad (4.17)$$

where $0 \leq \epsilon_4 \leq 1$. The value of ϵ_4 depends on the particular application and requires some experimentation. Too large a value produces oscillations which can diverge and too small a value converges too slowly. A value of 0.5 was found to work well for the example problem presented in Section 4.4 while values of 0.1 - 0.3 were used in the applications given in Chapter 6. Using Eq. (4.17), the control history assumed for the next pass is shown in Table III. Provided ϵ_4 is properly chosen, the results of the first iteration will not produce large changes in the controls and the error in the Number 2 switch $t_2^{*(1)} - t_2^{(1)}$ will be smaller than after the initial pass. This procedure of iteration on only switch 2 is continued until the error in this switch is below a specified level ϵ_3 . The

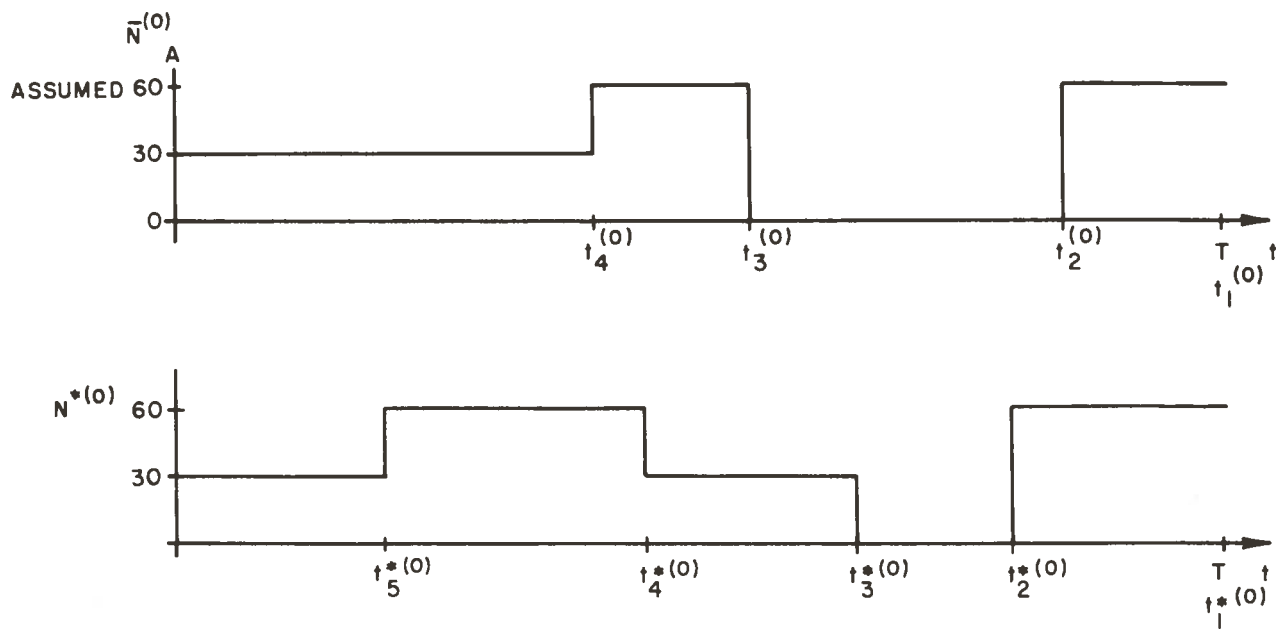


Figure 16.- Initial control histories

TABLE III.- ITERATION 1 ASSUMED CONTROL $\bar{N}^{(1)}$

SWITCH NUMBER	SWITCH TIME	$\bar{N}^{(1)}$
1	$t_1^{(1)} = T$	60
2	$t_2^{(1)} = t_2^{(0)} + \epsilon_4 (t_2^{*(0)} - t_2^{(0)})$	0
3	$t_3^{(1)} = t_3^{(0)}$	60
4	$t_4^{(1)} = t_4^{(0)}$	30

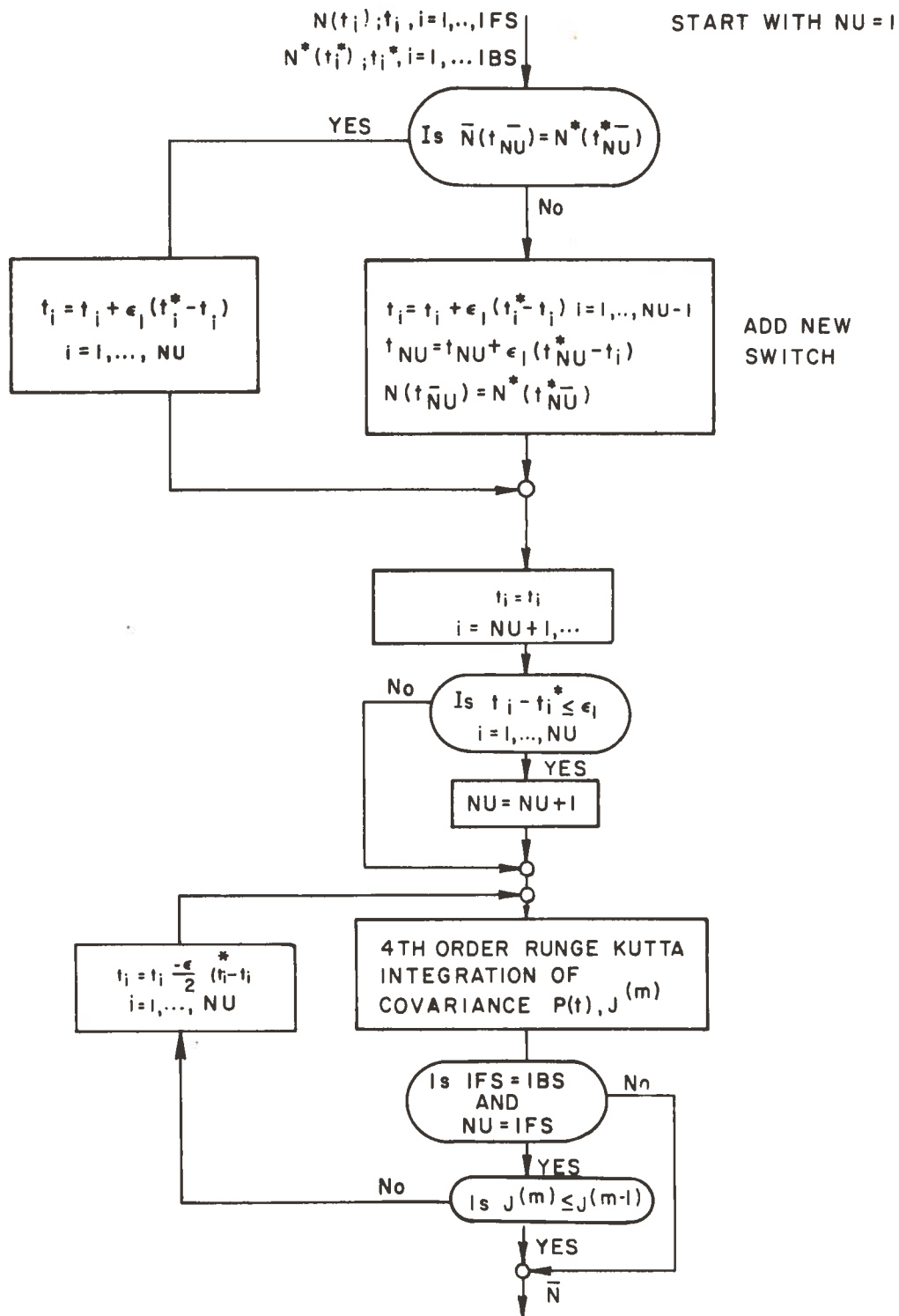


Figure 18.- Control iteration scheme

The linearized system dynamics F is:

$$F = \begin{bmatrix} 0 & 0 & 1 & 0 \\ 0 & 0 & 0 & 1 \\ 0 & 0 & 0 & 0 \\ 0 & 0 & 0 & 0 \end{bmatrix}$$

For the DME transmitters located at (90 nm, 20 nm) and (270 nm, -20 nm), the geometric sensitivity H is:

$$H = \begin{bmatrix} \frac{90-x}{D_1} & \frac{20-y}{D_1} & 0 & 0 \\ \frac{270-x}{D_2} & \frac{-20-y}{D_2} & 0 & 0 \end{bmatrix} \text{ NOM}$$

where D_1 and D_2 are the nominal ranges between the vehicle and the DME 1 and DME 2 transmitters.

The measurement errors are modeled (ref. 13) as:

$$R = \begin{bmatrix} (0.1 + 0.01 D_1)^2 \text{ nm}^2 & 0 \\ 0 & (0.1 + 0.01 D_2)^2 \text{ nm}^2 \end{bmatrix}$$

The environmental disturbances, as modeled in Appendix D:

$$Q = \begin{bmatrix} 0 & 0 & 0 & 0 \\ 0 & 0 & 0 & 0 \\ 0 & 0 & 0.0895 \frac{\text{nm}^2}{\text{hr}^3} & 0 \\ 0 & 0 & 0 & 32.0 \frac{\text{nm}^2}{\text{hr}^3} \end{bmatrix}$$

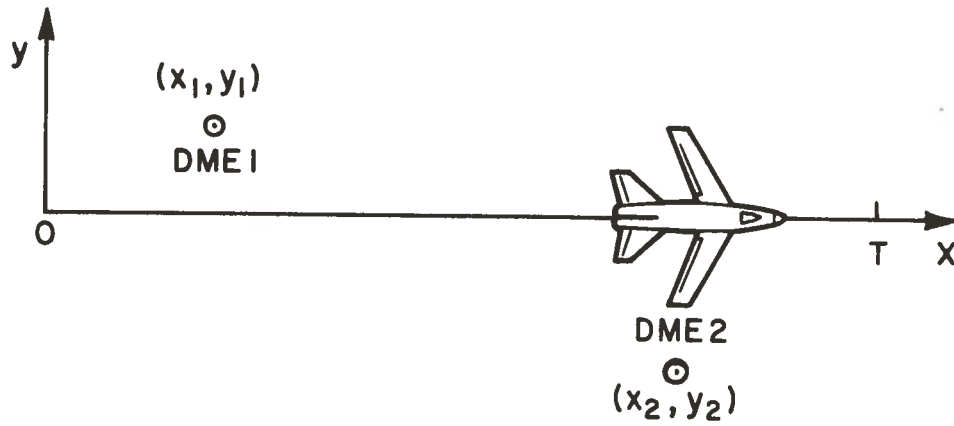


Figure 19.- System geometry

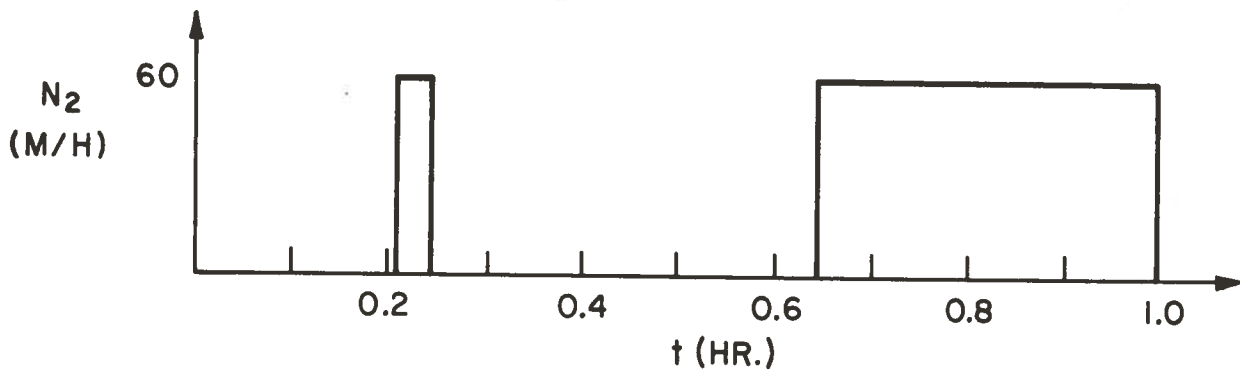
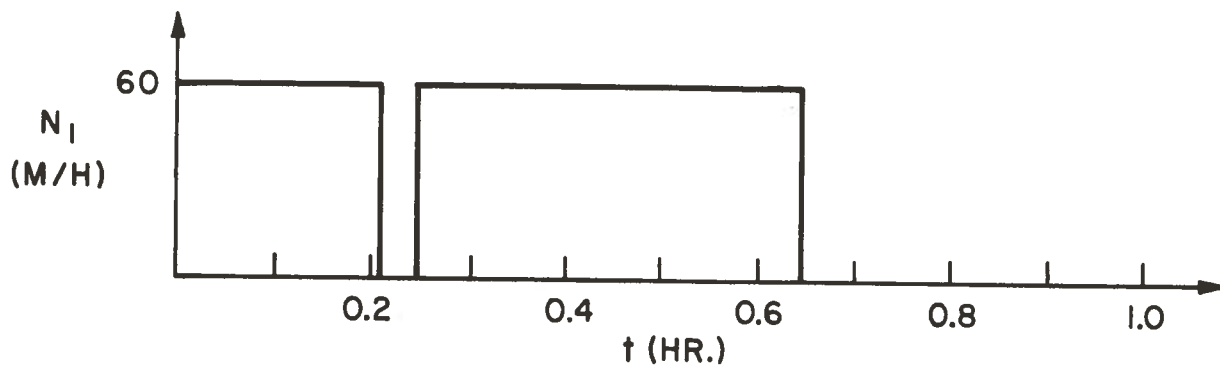


Figure 20.- Optimal measurement history

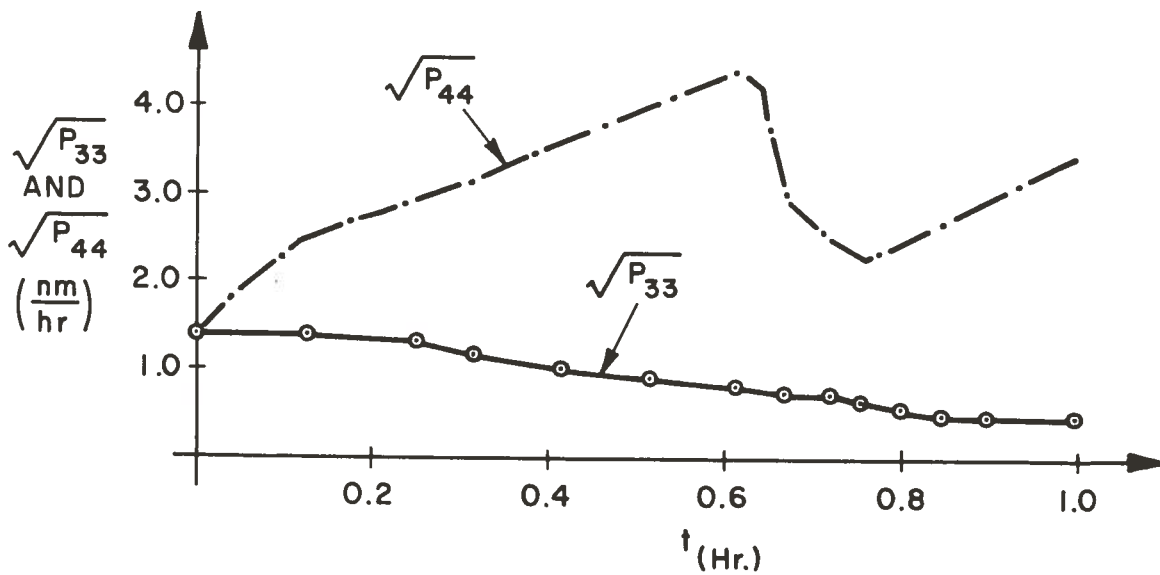
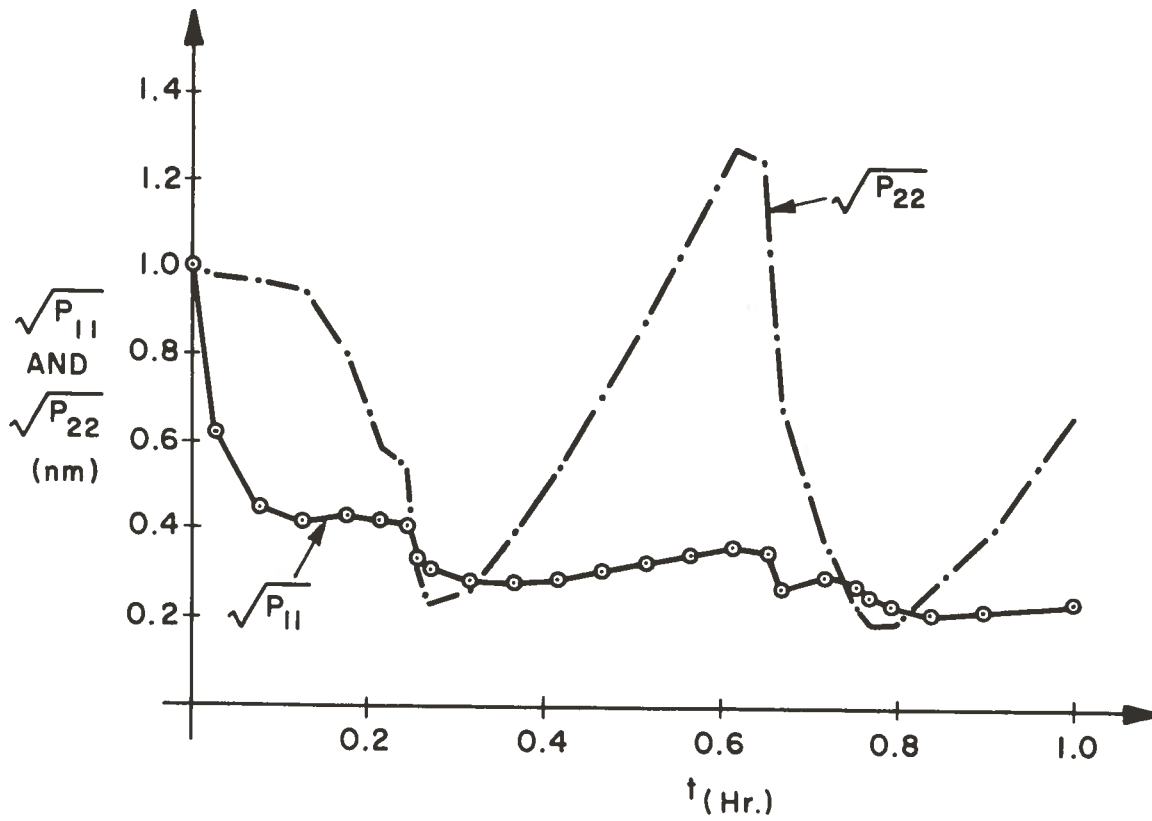


Figure 22.- RMS position and velocity estimation errors

solution. An assumed control was selected that ignored the computer constraint. This shall be referred to as the Limiting Case Solution, and will be discussed in Chapter 5. For this case, all sources are sampled at their maximum rates. For the example in this section, $N_1 = 60$ M/H and $N_2 = 60$ M/H. Integrating forward and backward produces a N^* . For the next iteration, N^* is used for the forward integration, i.e., $\bar{N}(1) = N^*(0)$. From this point on, the techniques of Section 4.3 are used to iterate on the individual switch times. This procedure was found very useful especially in cases where the regions in which the sensors produced good information have little overlap.

The effects of the iteration control parameters ϵ_3 , ϵ_4 , and ϵ_5 and the sensitivity of the solution are inter-dependent. The set of parameters used in the example problem are given in Table VI. ϵ_3 determines how well a t_i and t_i^* must match before t_{i+1} can be iterated. ϵ_4 is the fraction of the error ($\bar{N} - N^*$) used to update \bar{N} . ϵ_5 is the limit that defines convergence; i.e., if $|t_i - t_i^*| < \epsilon_5$ for all i , then convergence is declared. There are two types of solution sensitivity. The first type is when the parameters of the application (sensor accuracies, environmental disturbances, and geometry) are such that the optimal switching functions have regions where the switching functions for two or more sensors are almost equal. In such cases, the optimization procedure will oscillate between two control histories which have a different number of switch points. An example of this behavior is shown in Figure 23 (Mode B). This corresponds to the example given in this section with environmental disturbances $\sigma_v = 2.5$ fps. The optimal control logic states that if the switching functions are equal then either sensor can be used. For the optimization procedure to converge to a solution for such cases, the step size, ϵ_4 , should be reduced and the convergence limit, ϵ_5 , relaxed. When $\epsilon_4 = 0.3$ and $\epsilon_5 = 0.002$ hr were used, the procedure produced solution (A). The form of the optimal measurement histories appears to be dependent on the values of the ϵ 's. This is not disturbing because the value of the performance index (which is the important quantity) using either switching Mode (A) or (B) is the same to five decimal places.

TABLE VI.- CONTROL ITERATION PARAMETERS

$\epsilon_3 = 0.005$ hr
$\epsilon_4 = 0.5$ (Nondimensional)
$\epsilon_5 = 0.001$ hr

Chapter 5

DESIGN PROCEDURE

5.1 INTRODUCTION

The object of this section is the detailed development of an efficient and flexible set of logic to provide the system designer with system design and utilization data. This logic is called the design procedure. The data generated by the design procedure will be utilized by the designer to select the "best" navigation system. The design procedure, shown in Figure 24, starts with the list of candidate sensors and computers and with the system performance requirements. This data is operated on by one of three design options. Each option (Figure 25) contains a selection logic which determines the order in which the candidate systems are evaluated and a set of techniques for evaluating the systems. The output of this procedure includes the results of the selected design option plus auxiliary data selected by the designer. The emphasis in this development is on the generation of efficient logic as opposed to the presentation of an efficient computer program. For this reason no computer program listing is included. Detailed logic flow charts are included in sufficient detail so that an interested reader can write a program using these flow charts.

The techniques used to evaluate a system are essentially the same for each of the three design options and will be presented first. Next, the design options and the selection logic for each option are discussed. Finally, a discussion is given of the auxiliary data available to the designer. The combination of selection and evaluation logic plus the auxiliary data forms an efficient and flexible design tool.

5.2 EVALUATION TECHNIQUES

Before discussing the system evaluation logic it is useful to define two terms. First, candidate systems refers throughout the discussion to the set of $(2^n - 1) \times C$ possible systems, corresponding to the n candidate sensors and the C candidate computers. Also, the Optimization Technique refers to the technique developed in Chapter 4 for the determination of the optimal measurement schedule and the minimum value of the system performance index.

To evaluate the candidate systems, it is possible to apply the Optimization Technique to all systems. It is recognized, however, that this requires a good deal of computation, and thus to improve the efficiency of the design procedure, a second level of evaluation analysis, the Limiting Case Analysis, is introduced

(Figure 26). This analysis makes use of an open loop integration of the covariance matrix equation

$$\dot{P} = FP + PF^T - PH^TNR^{-1}HP + Q \quad (5.1)$$

using selected measurement histories $N(t)$.

To illustrate the techniques used to select the $N(t)$ and to investigate the physical meaning of these control histories, consider a simple example.

Table VII presents the characteristics of the two candidate sensors and the three candidate computers considered in this example. (Assume that these sensors are single-source type sensors). The total number of configurations to be analyzed is $(2^2 - 1) \times 3 = 9$. On examination of the data in Table VII, it can be recognized that the optimal measurement schedule for seven of the nine configurations can be determined by inspection. These configurations and their optimal measurement schedules are given in Table VIII. The optimal schedule can be determined by inspection for two reasons. First, for a single sensor configuration the optimal switching law requires that the use of that sensor be limited by either the computation limit or physical sampling limit. In the present example, the optimal schedules for the single-sensor systems, S1-C1 and S2-C1, are determined by the processing constraint while the schedules for systems S1-C2, S2-C2, S1-C3, and S2-C3 are determined by the sensor sampling constraints. The second situation arises when the limiting factor for multi-sensor systems such as S1-S2-C3 is the sensor sampling constraints. In this situation, the computer does not limit the sampling rates. Both types of limitations usually occur for systems with a small number of sensors. To evaluate the performance of such systems, the optimal $N(t)$ given in Table VIII are used to integrate Eq. 5.1 from $t = 0$ to $t = T$. Then the optimal value of the system performance $J = \text{tr} [AP(T)]$ is computed.

Of the original nine configurations, only two systems, S1-S2-C1 and S1-S2-C2, require further investigation. Consider the system S1-S2-C2. The admissible control region for this system is shown in Figure 27. The optimal measurement schedule does not correspond to any one point on this figure but rather to a switching between points A and B. To determine the times at which these switches occur would require the application of the Optimization Technique. It can be seen, however, that although point C is not an admissible control point due to the violation of the computer constraint, the following relation is true

TABLE VII
CANDIDATE SENSORS

Sensor Number	Maximum Sampling Rate (M/H) *	Relative Computer Loading
S1	60	1
S2	60	1

CANDIDATE COMPUTERS

Computer Number	Computer Capacity (M/H) *
C1	50
C2	90
C3	150

* M/H = Measurements/hour

TABLE VIII
OPTIMAL SCHEDULE OF MEASUREMENTS

SYSTEM CONFIGURATION	OPTIMAL MEASUREMENT SCHEDULE (MPH)
1. S1 - C1	$N_1 = 50$
2. S1 - C2	$N_1 = 60$
3. S1 - C3	$N_1 = 60$
4. S2 - C1	$N_2 = 50$
5. S2 - C2	$N_2 = 60$
6. S2 - C3	$N_2 = 60$
7. S1 - S2 - C3	$N_1 = 60; N_2 = 60$

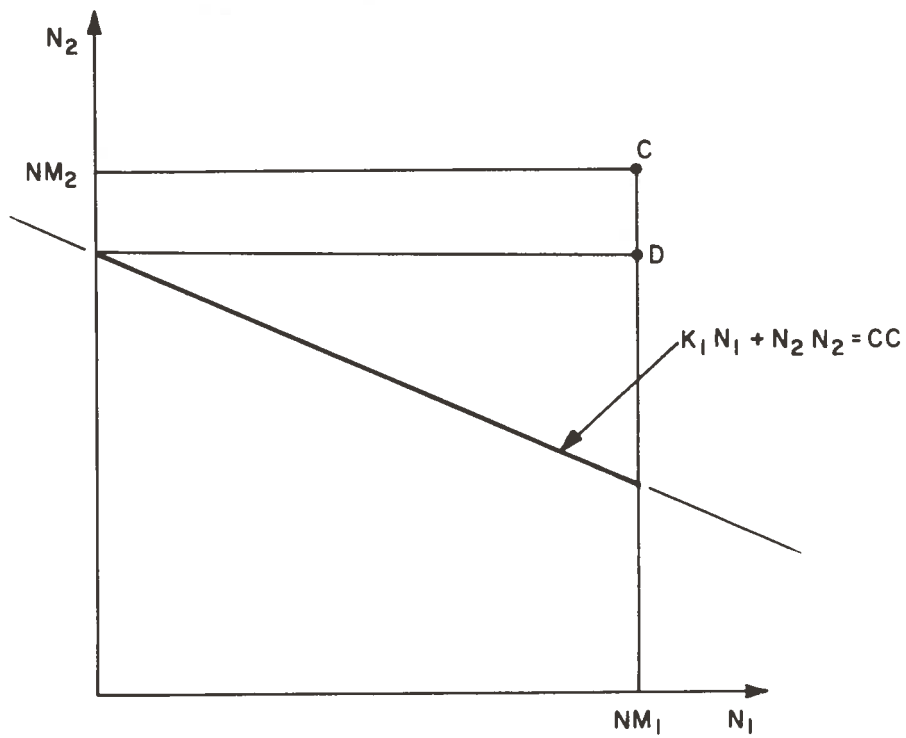


Figure 28.- Admissible control region

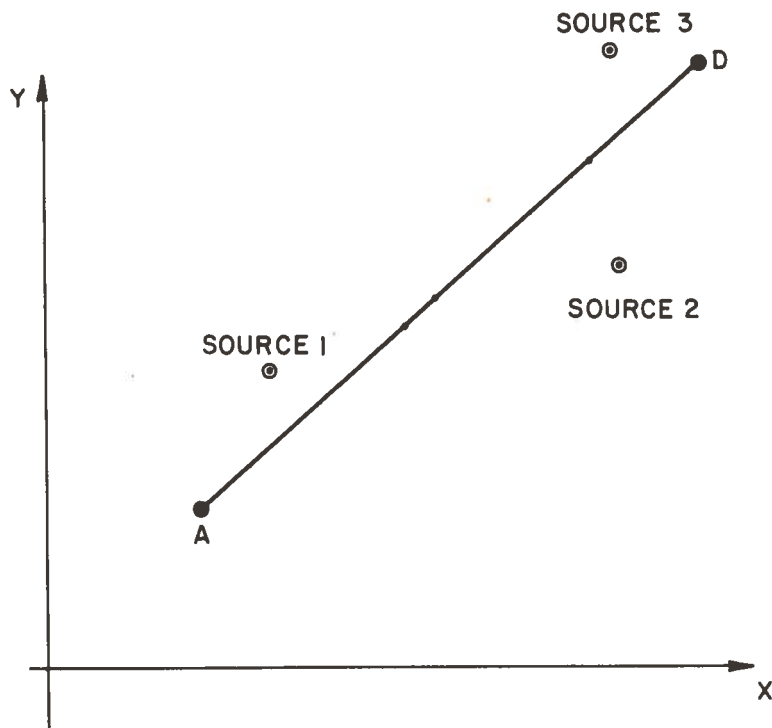


Figure 29.- Multiple source geometry for sensor 2

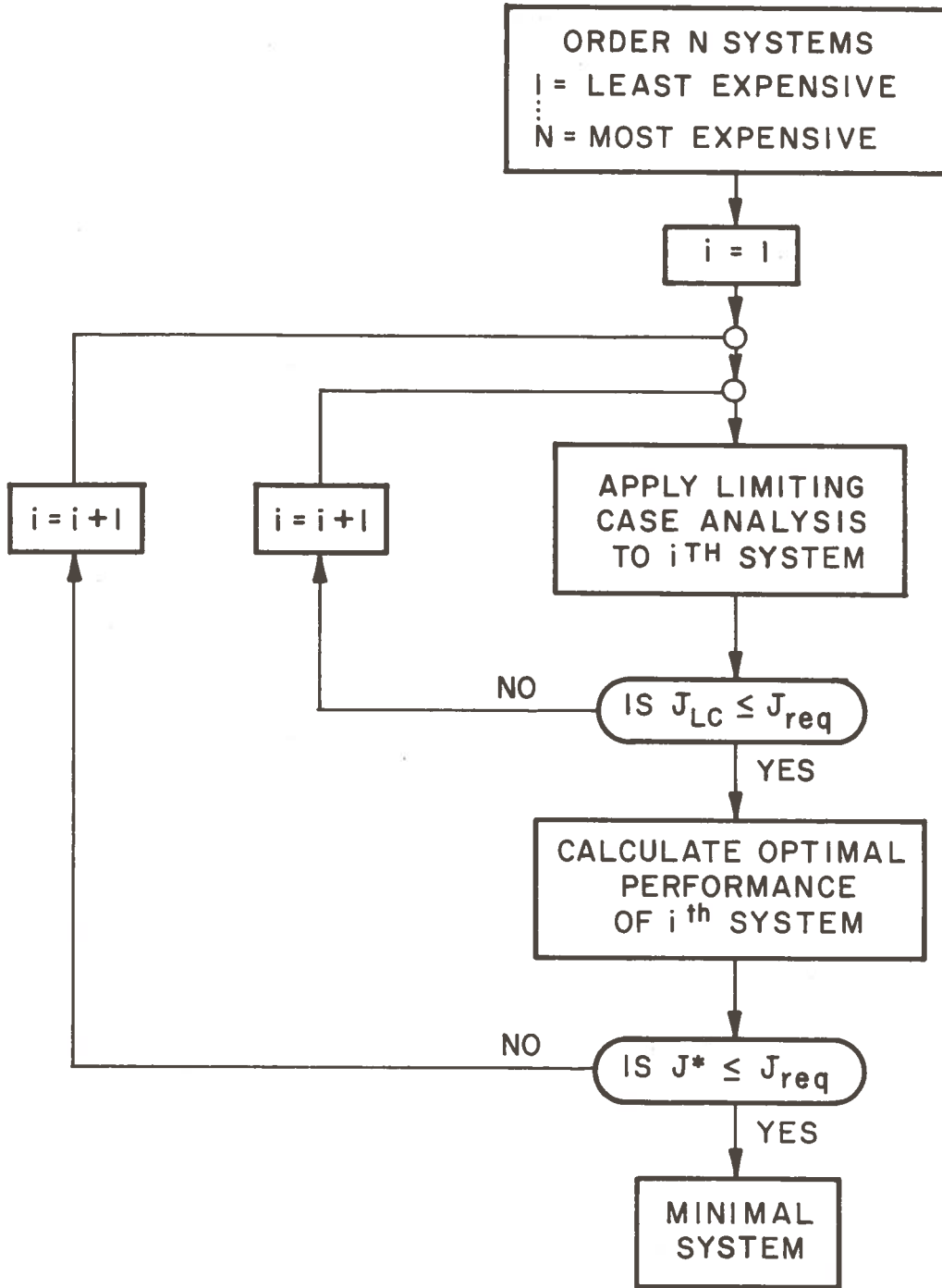


Figure 30.- Minimal system selection and evaluation logic

to the next system in the order. The first system which has a $J^* \leq J_{Req}$ is the Minimal system.

This logic is efficient, not only due to the use of Limiting Case Analysis, but also due to the order of selection from least expensive to most expensive. At each stage, the process has the possibility of eliminating all systems which occur further down in the order.

5.3.2 Set of Minimal Systems

The second design problem, which is more complicated than the Minimal System design option, is the determination of the set of Minimal Systems. To explain this option, it is necessary to define some terms. A sensor chain is defined as the list of all configurations that include a particular sensor. A Computer chain is defined in an analogous fashion. For n sensors and c computers each sensor chain has $2^{n-1} \times C$ systems and each computer chain has $(2^n - 1)$ systems. Table X shows the 4 chains corresponding to 2 candidate sensors and 2 candidate computers. For each chain, there may be a Minimal System. The set of Minimal Systems is the list of those local minimal. The overall Minimum System is seen to be a subset of this list. The information provided by this option is useful if, for reasons other than system accuracy or cost, it is desirable to either use or eliminate a particular sensor or computer from the list of candidate elements. An example of this would be if the designer lacks confidence in the ability of a vendor to deliver a particular sensor according to schedule, he may decide not to choose any configuration which uses that sensor. To insure a comparison

TABLE X

Candidate Sensors - S1, S2

Candidate Computers - C1, C2

S1 Chain	S2 Chain	C1 Chain	C2 Chain
S1-C1	S2-C1	S1-C1	S1-C2
S1-C2	S2-C2	S2-C1	S2-C2
S1-S2-C1	S1-S2-C1	S1-S2-C1	S1-S2-C2
S1-S2-C2	S1-S2-C2		

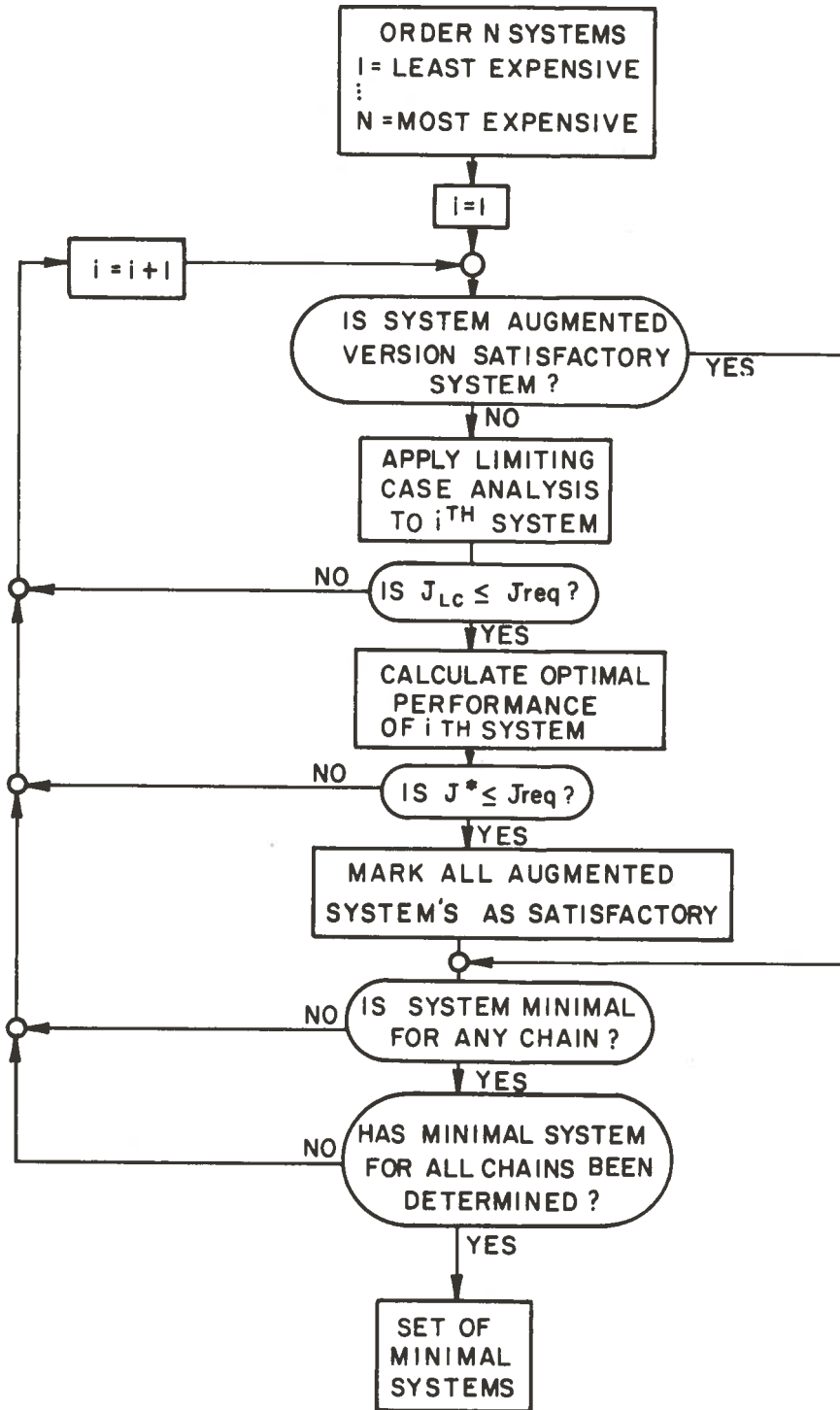


Figure 31.- Set of minimal systems selection and evaluation logic

TABLE XI

ORDER SYSTEM AND CHAIN COST LISTINGS

ORDERED SYSTEM COST LIST	
1. DME-C1	(16) *
2. DME-C2	(46)
3. Doppler-C1	(50)
4. DME-Doppler-C1	(56)
5. Doppler-C2	(80)
6. DME-Doppler-C2	(86)

ORDERED SENSOR AND COMPUTER CHAINS COST LISTS			
DME-Chain	Doppler-Chain	C1-Chain	C2-Chain
1. DME-C1 (16) *	1. Doppler-C1 (50)	1. DME-C1 (16)	1. DME-C2 (46)
2. DME-C2 (46)	2. DME-Doppler-C1 (56)	2. Doppler-C1 (50)	2. Doppler-C2 (80)
3. DME-Doppler-C1 (56)	3. Doppler-C2 (80)	3. DME-Doppler-C1 (56)	3. DME-Doppler-C2 (86)
4. DME-Doppler-C2 (86)	4. DME-Doppler-C2 (86)		

* System Cost in dollars x 10³

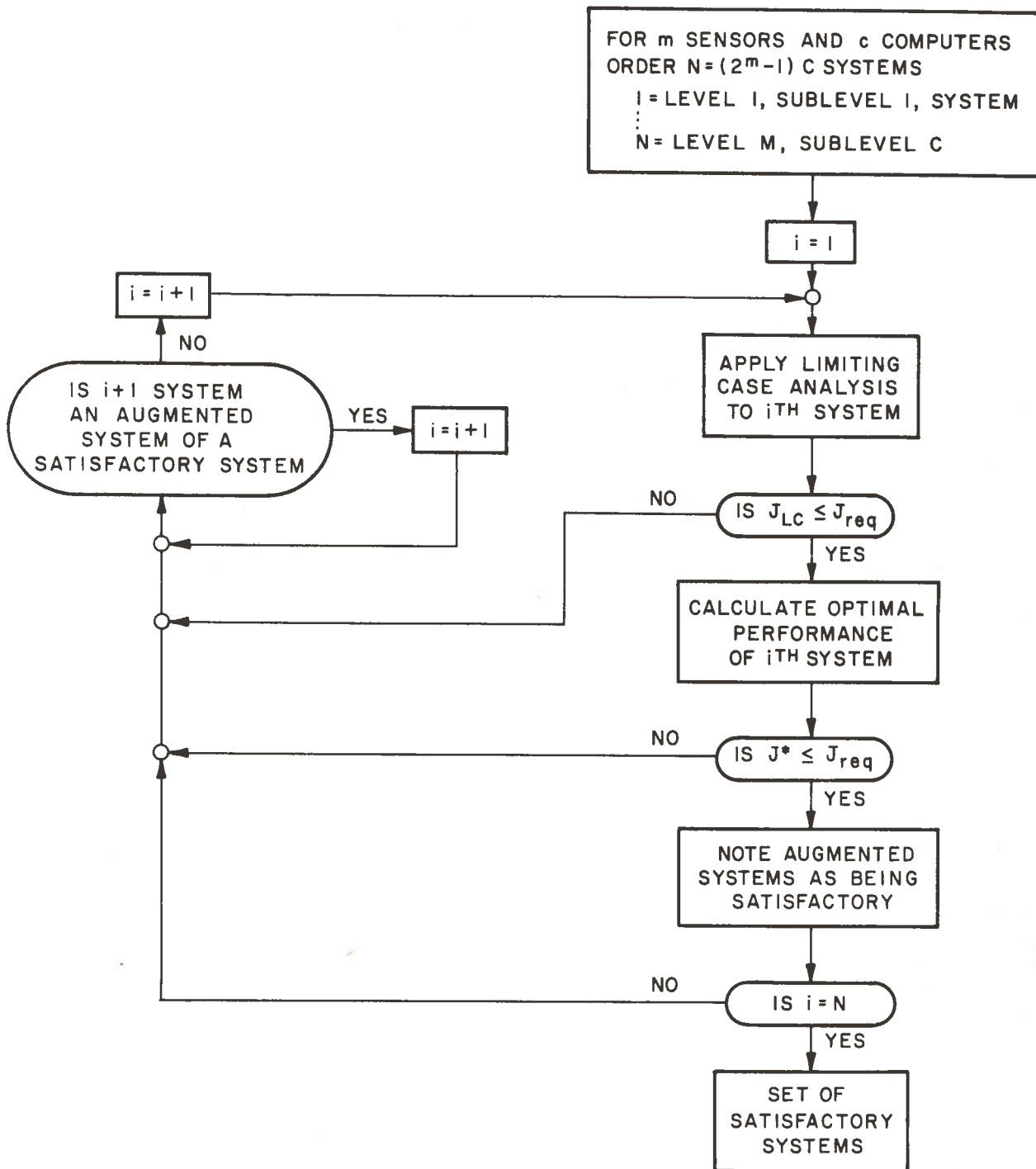


Figure 32.- Selection and evaluation logic for determination of satisfactory systems

individual sensor. The resulting performance index was a measure of the basic capabilities of the sensors in the configuration. A comparison of this result with the results of using the Optimization Technique is a direct indication of the impact of the computer on the effectiveness of the system. For example, consider the case of a system made up of a DME sensor (which measures range from a DME transmitter) and a very High Frequency Omnidirectional Radio Range (VOR) sensor (which measures magnetic bearing of the receiver from the VOR transmitter) and a computer which allows only one sensor to operate at a time. This system is used in an aircraft whose flight path is as shown in Figure 33. The results of the Limiting Case Analysis were $J = P_{11}(T) = 0.3982 \text{ nm}^2$ and the optimal performance was $J = 0.4108 \text{ nm}^2$. This indicates that a doubling in computer capacity produces virtually no improvement in the system performance index. Physically speaking, the sensors and not the computer are the limiting factors. For this simple case, this is anticipated since the regions in which each sensor produces good information have virtually no overlap. For more complicated systems, this same line of reasoning can be applied even though system complexity may rule out a correct intuitive guess.

A second class of data which is available from the application of the Optimization Technique consists of the time histories of the estimation error covariance matrix. Although only the values of this covariance at the terminal time are included in the performance index, the behavior of the elements of $P(t)$ at times between $t = 0$ and $t = T$ may be used in the design selection. As an example, consider the time histories of the root mean squared (RMS) position uncertainty for two systems shown in Figure 34. Although they both have approximately the same RMS value at $t = T$, System 1 goes through a region where little information is received and therefore, the uncertainty builds up in this region. Based on the application at hand, this may or may not be important. With such data, however, the designer can make his decision.

A third set of data is sensitivity data. This kind of data is developed only for the computer because this is the only part of the system in which changes in characteristics are meaningful. For example, a ten-percent change in the measurement accuracy of a sensor would most likely require the development of a new sensor which would not be available in time to be used. Also a small change in the location of a ground transmitter does not make sense. It does make sense in some cases to consider a ten-percent change in computer capacity. This might correspond to a slight adjustment of the computer budget. There are two forms of computer sensitivity: one which is analytic in nature and applies only for a small change in computer capacity CC , and one which is developed by repeated application of the Optimization

Technique. Consider first the analytic sensitivity. Figure 35 shows the flight path and source geometry for a system which has two DME receivers. DME1 is tuned to receive information only from source 1 and DME2 can receive information only from source 2. Also shown are the optimal measurement schedules for two computers $cc = 60$ M/H and $CC = 90$ M/H. Two effects of the increase in computation capacity on the control histories can be seen. First the level of the sensor not on its boundaries has changed from zero to thirty M/H as would be expected. The second difference is that the time of the switch in measurement rates has changed. This change is relatively small considering that the computer capacity has been increased by 50 percent. For smaller changes in CC , it is anticipated that this difference would be still smaller. Therefore, it is assumed that for small changes in computer capacity ΔCC the change in the control history is approximated by leaving all switch times unchanged and using $\Delta N_i = \Delta CC$ for the sensor not on its limit. Applying this logic to Case A in Figure 35 the change in the control is given by:

$$\begin{aligned}
 0 < t \leq t_1 & \quad \Delta N_1 = 0 \quad ; \quad \Delta N_2 = \Delta CC \\
 t_1 < t \leq T & \quad \Delta N_1 = \Delta CC \quad ; \quad \Delta N_2 = 0
 \end{aligned}
 \tag{5.4}$$

In Appendix F, the expression for the first-order variation in system performance index δJ due to a first order variation in the control histories δN is given by:

$$\delta J = - \left[\int_0^T \sum_{i=1}^m \left(R^{-1} H P \phi^T A \phi P H^T \right)_{ii} \delta N_{ii} dt \right]_{cc_0}
 \tag{5.5}$$

where the time histories of P , ϕ , H , and R correspond to the optimal $N(t)$ which had a computer constraint of CC_0 . ϕ is the transition matrix which satisfies the equation:

$$\dot{\phi} = \phi \left(F - P H^T N R^{-1} H \right)
 \tag{5.6}$$

with

$$\phi \left(T, T \right) = I$$

Assuming that $\delta N = \Delta N$ as given by Eq. 5.4 the change in J for small change ΔCC about CC_0 is given by

$$\delta J = \left[- \int_0^{t_1} \left(R^{-1} H P \phi A \phi^T P H^T \right)_{22} \Delta CC \, dt \right. \\ \left. - \int_{t_1}^T \left(R^{-1} H P \phi A \phi^T P H^T \right)_{11} \Delta CC \, dt \right]_{CC_0} \quad (5.7)$$

Therefore:

$$\frac{\delta J}{\Delta CC} = - \left[\int_0^{t_1} \left(R^{-1} H P \phi A \phi^T P H^T \right)_{22} \, dt \right. \\ \left. + \int_{t_1}^T \left(R^{-1} H P \phi A \phi^T P H^T \right)_{11} \, dt \right]_{CC_0} \quad (5.8)$$

Equation 5.8 provides the designer with a measure of the effect of increased computer capacity. If this were to indicate a large return for a small increase in CC, it would be beneficial to adjust the computer budget slightly to accommodate this change.

A second form of the sensitivity of the system performance index J for various computer capacities can be generated by repeated applications of the Optimization Technique. The results of this analysis would be a curve similar to that shown in Figure 36. Point A corresponds to the situation in which no measurements are taken. The value of J for this case can be determined by direct integration of

$$\dot{P} = FP + PF^T + Q \quad (519)$$

with

$$P(t_0) = P_0$$

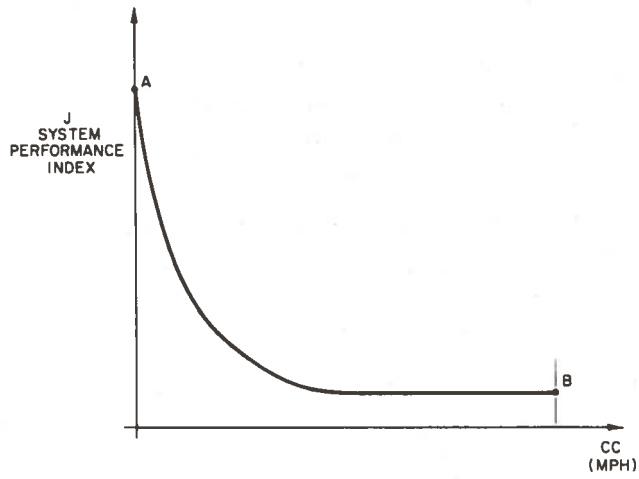


Figure 36.- Sensitivity of the performance index J

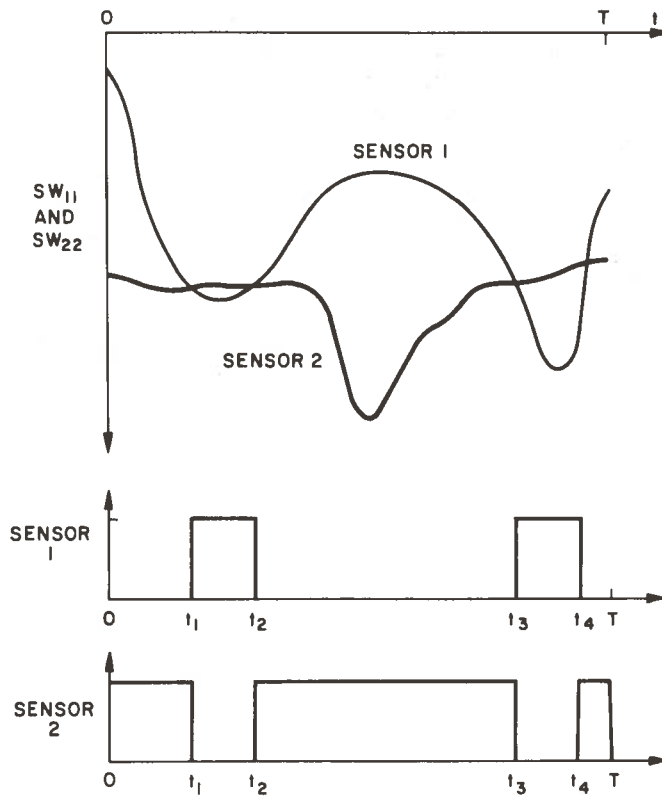


Figure 37.- Typical switching functions and corresponding measurements histories

Chapter 6

AVIONICS SYSTEM DESIGN

6.1 INTRODUCTION

To illustrate the characteristics of the Design Procedure, an example problem is now presented. This example considers the design of an aircraft cruise navigation system. Starting with a given problem statement, the engineering formulation is developed and the candidate components selected. All three design options are then applied to the design and the results of each option are presented and discussed. Also presented is a summary of the analysis used in generating the output of all three options. A list of all 45 candidate systems arranged in order of cost is given in Appendix G. Included in this appendix is a summary of the analysis and performance for all systems evaluated.

6.2 PROBLEM STATEMENT AND CONVERSION TO ENGINEERING TERMS

The designer is presented with the following assignment. "Design the best cruise navigation system for a V/STOL Airbus type operation between Boston and Washington, D.C. This system should arrive at its destination with position uncertainties no greater than 0.25 nm."

Converting this problem into engineering terms results in the following data.

6.2.1 Mission Data

The nominal trajectory was chosen as a straight line path between Boston and Washington, D.C. (Figure 38). The cruise altitude was selected as 20,000 ft, and the vehicle chosen was a modification of the XC-142 experimental tilt wing V/STOL aircraft. The characteristics of this vehicle (ref. 19) are given in Table XIII. The flight environment was taken as a random isotropic gust field with root-mean-squared gust of 2 fps (ref. 18) and a correlation time of 0.471 sec (ref. 20). Using the vehicle characteristics, the resulting acceleration perturbations were derived using the analysis given in Appendix E. They are:

$$Q_{33} = 0.358 \text{ nm}^2/\text{hr}^3$$

$$Q_{44} = 128.0 \text{ nm}^2/\text{hr}^3$$

TABLE XIII.- VEHICLE CHARACTERISTICS

Cruise Velocity = 360 nm/hr
Wing Area = 535 ft ²
Side Area = 830 ft ²
Gross Weight = 38,000 lbs
Cruise L/D = 7.3
$C_{Y\beta} = 1.03$

6.2.2 Mission Objective

The mission objective is arrival at the terminal point with an uncertainty in position no greater than 0.25 nm. Considering this, the performance index was chosen as:

$$J = P_{11}(T) + P_{22}(T)$$

where P_{11} is the mean-squared uncertainty in the x (along track) direction, and P_{22} is the mean-squared uncertainty in the y (cross-track) direction.

6.2.3 System Data

The characteristics of candidate sensors and computers are given in Table XIV. Costs are given for the on-board equipment (refs. 13, 15). These 4 sensors were selected because of the general availability of this information in the Northeast Corridor. The ground network of information transmitters was taken to be three VORTAC stations which transmit both VOR bearing and DME range information from each site, and a Decca chain made up of one master and three slave transmitters. The locations of the ground transmitters are given in Table XV. The sensor sampling limits NM_i are taken as the availability of the transmitted data. The computers used do not correspond to any specific existing machines but represent a range of available computers.

An interesting fact that can be seen upon examination of the sensor and computer data given in Table XIV is that the rates at which the sensors will be sampled in the system are limited

6.3 DESIGN PROCEDURE RESULTS

The results of exercising all three design options of the Design Procedure are presented for the problem defined in Section 6.2. The desired output from each option, plus a summary of the analysis performed are given for each option. In addition, auxiliary design data is presented for the Minimal System Option. In the analysis summaries, the following abbreviations are used.

L.C. = Limiting Case Analysis

O.T. = Optimization Technique

A.S. = Augmented System Concept

Also, when the Augmented System Concept is applied, the system performance is only bounded. This is indicated by the less than inequality symbol (<).

6.3.1 Minimal System

To determine the Minimal System, the two analysis techniques (Limiting Case and Optimization) were applied to the candidate systems, starting with the least expensive system and working down the cost listing. The first system which satisfies the performance requirement is the Minimal System.

The Minimal System for the present design problem was the VOR-DME-C3 system which has the following characteristics.

Minimal Configuration: VOR-DME-C3

Optimal Terminal Position Uncertainty: 0.2265 nm

Limiting Case Terminal Position Uncertainty: 0.1921

Systems Cost: \$69,000

Determining this Minimal System required 25 applications of the Limiting Case Analysis and 9 applications of the Optimization Technique. A summary of this analysis is given in Table XVI.

An examination of the data in Table XVI shows a second system that misses satisfying the performance requirement by a small amount but has a smaller cost. This system (DME-Doppler-C1) warrants further examination. Two other systems (Nos. 15 and 23) also show a terminal uncertainty only slightly larger than that which is required. These systems are, however, augmented versions of the DME-Doppler-C1 system, and show very small reductions

TABLE XVI (Continued)

SYSTEM NO.	CONFIGURATION	COST \$ x 10 ³	PERFORMANCE (nm)	ANALYSIS	ADDITIONAL DATA
14	Decca-C2	54	0.8616	L.C.	This is also optimal value
15	DME-VOR-Doppler-C1	57	0.2505	O.T.	Limiting Case 0.1761 nm.
16	VOR-Decca-C2	58	0.3068	L.C.	
17	DME-Decca-C2	59	0.3360	L.C.	
18	Doppler-Decca-C1	62	0.3763	L.C.	
19	DME-VOR-Decca-C2	63	0.2827	O.T.	Limiting Case 0.2349 nm.
20	VOR-C3	64	0.2585	O.T.	Limiting Case 0.2499 nm.
21	DME-C3	65	0.3176	L.C.	
22	VOR-Doppler-Decca-C1	66	0.3377	O.T.	Limiting Case 0.2402 nm.
23	DME-Doppler-Decca-C1	67	0.2506	O.T.	Limiting Case 0.1941 nm.
24.	Doppler-C2	68	1.4679	L.C.	This is also optimal value
25	DME-VOR-C3	69	0.2265	O.T.	Limiting Case 0.1921 nm.

in terminal uncertainty while having higher cost than the DME-Doppler-C1 system. For these reasons, only the DME-Doppler-C1 system will be examined further. The characteristics of this system are as follows.

Configuration: DME-Doppler-C1

Optimal Terminal Position Uncertainty: 0.2509 nm

Limiting Case Terminal Position Uncertainty: 0.1921 nm

System Cost: \$53,000

This system could be an acceptable design if either the design specifications were relaxed or if a small increase in computer capacity (a change in computer budget not a change of machines) gave a terminal uncertainty less than or equal to 0.25 nm. To investigate the latter possibility, a trade off of Mean-Squared Terminal Position Uncertainty versus computer capacity (CC) was performed. This tradeoff (Figure 39) was generated by application of the Optimization Technique for DME-Doppler systems with CC = 120, 180, 240, and 360 (M/H). This curve shows that an increase of only 3 percent in CC is required.

To aid the designer in his selection of which of these two systems (VOR-DME-C3 and DME-Doppler-C1) he should investigate in more detail, additional data were generated for both systems. These data are the time histories of the optimal control and RMS position and velocity estimation errors. These curves are shown in Figures 40 and 41 for the VOR-DME-C3 systems and in Figures 42 and 43 for the DME-Doppler-C1 system.

6.3.2 Set of Minimal Systems

The set of Minimal Systems and their characteristics are given in Table XVII. To arrive at this list required the use of the Limiting Case Analysis 31 times; the application of the Optimization Technique to 12 systems, and the use of the Augmented System concept once. A summary of this analysis is shown in Table XVIII. An examination of this data shows, as discussed in Section 6.3.1, that if C1 is enlarged slightly the DME-Doppler-C1 system (System No. 13) and all the augmented versions of this system would satisfy the performance specifications. For this reason, a second set of Minimal Systems given in Table XIX, was generated. The two sets are referred to as Option A in which no enlargement of C1 is allowed and Option B in which such an enlargement is permitted.

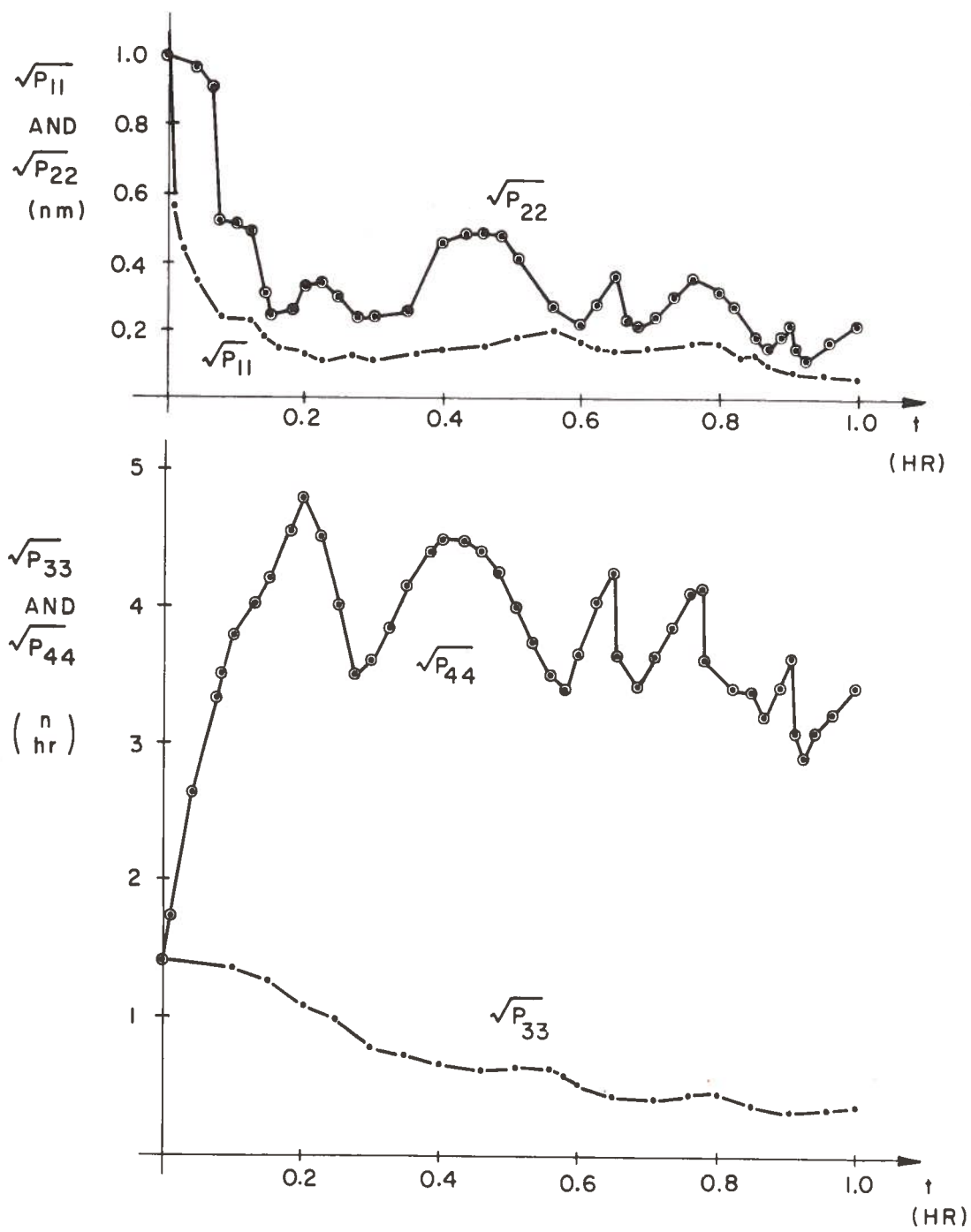


Figure 41.- RMS position and velocity estimation errors for VOR-DME-C3 system

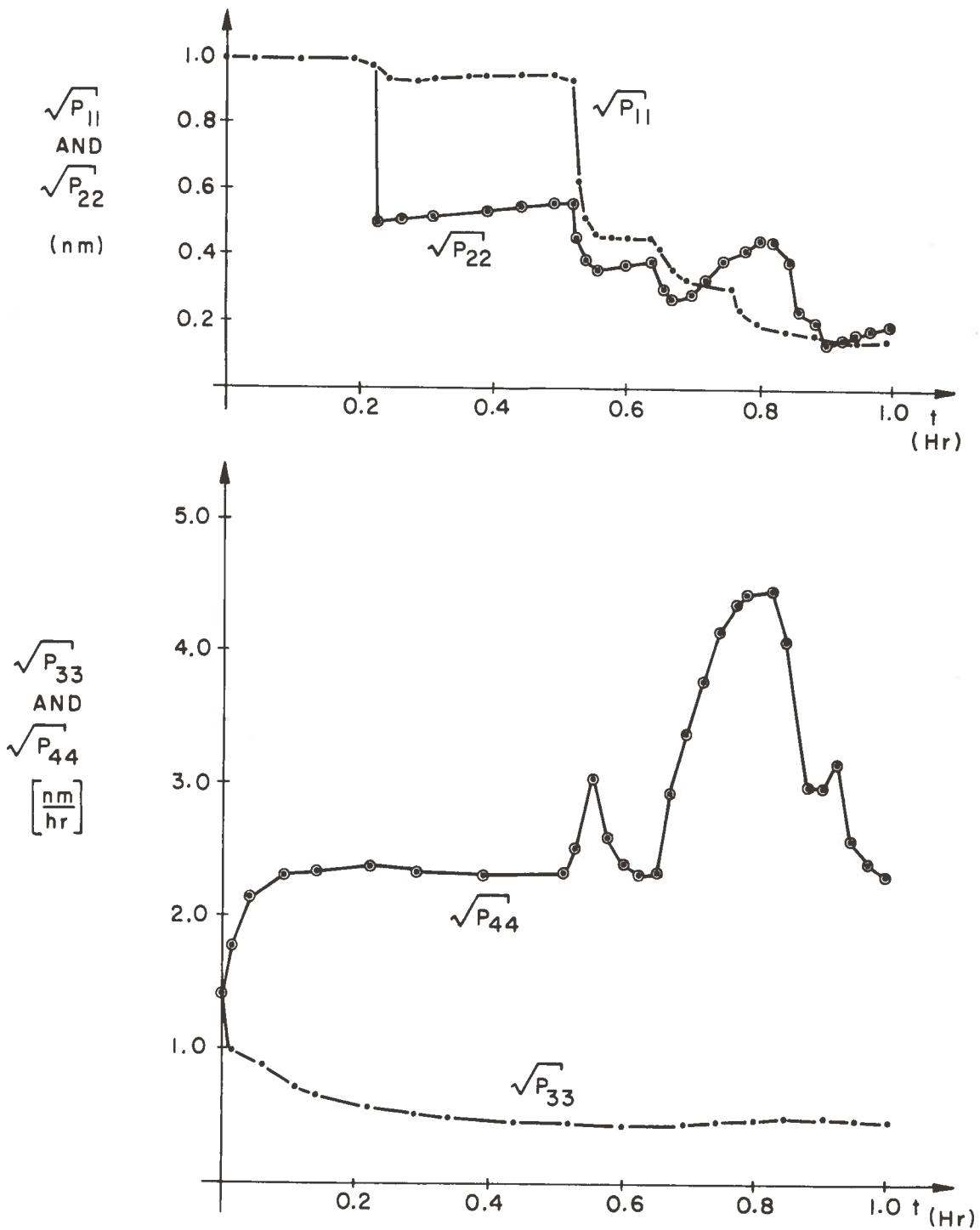


Figure 43.- RMS position and velocity estimation errors for DME-Doppler-CI system

TABLE XVIII

ANALYSIS SUMMARY FOR SET OF MINIMAL SYSTEMS OPTION

SYSTEM NO.	CONFIGURATION	COST \$ X 10 ³	PERFORMANCE (nm)	ANALYSIS	ADDITIONAL DATA
1	VOR-C1	24	0.4153	L.C.	
2	DME-C1	25	0.4097	L.C.	
3	VOR-DME-C1	29	0.2980	L.C.	
4	Decca-C1	34	0.9308	L.C.	This is also optimal value
5	VOR-Decca-C1	38	0.3727	L.C.	
6	DME-Decca-C1	39	0.3204	L.C.	
7	DME-VOR-Decca-C1	43	0.2919	L.C.	
8	VOR-C2	44	0.3214	L.C.	
9	DME-C2	45	0.3610	L.C.	
10	Doppler-C1	48	1.5183	L.C.	This is also optimal value
11	DME-VOR-C2	49	0.2828	O.T.	Limiting Case 0.2405 nm
12	VOR-Doppler-C1	52	0.3405	O.T.	Limiting Case 0.2493 nm

TABLE XVIII (Continued)

SYSTEM NO.	CONFIGURATION	COST \$ X 10 ³	PERFORMANCE (nm)	ANALYSIS	ADDITIONAL DATA
24	Doppler-C2	68	1.4679	L.C.	This is also optimal value
25	DME-VOR-C3	69	0.2265	O.T.	VOR, DME, C3 Min. Syst. Syst. Option A Limiting Case 0.1921 nm
26	DME-VOR-Doppler-Decca-C1	71	0.2504	O.T.	Limiting Case 0.1750 nm
27	VOR-Doppler-C2	72	0.2467	O.T.	Limiting Case 0.1781 nm
28	Decca-C3	74	0.6963	L.C.	This is also optimal value
29	VOR-Decca-C3	78	0.2582	O.T.	Limiting Case 0.2409 nm
30	DME-Decca-C3	79	0.2937	L.C.	
31	Doppler-Decca-C2	82	0.2688	L.C.	
32	DME-VOR-Decca-C3	83	< 0.2265	A.S.	Limiting Case 0.1891 nm Decca Min. Syst. for Option A

From the lists of the minimal systems, the designer can easily identify the overall Minimal System. It is also possible to see the gains or penalties associated with demanding that a particular sensor or computer be used or rejected. For example, in Option B, a Decca sensor requirement gives a system cost of \$14,000 higher than the DME-Doppler-C1 system, and a terminal RMS position uncertainty of 0.2506 nm, as compared to 0.2509 nm. It is evident that inclusion of Decca would be an inefficient choice. The inefficiency of Decca for this application is due to the fact that its information is limited to a small region early in the flight.

6.3.3 Satisfactory Systems

Of a total of 45 candidate systems identified at the start of the problem, 15 were found to be satisfactory. If the enlargement of the computer C1 is allowed, an additional four systems are satisfactory. A listing of the satisfactory systems ordered according to cost is given in Table XX. To derive this list required the following analyses:

- Limiting Case Analysis - 34 systems
- Optimization Technique - 14 systems
- Augmented System Concept - 11 systems

A summary of the analysis is given in Table XXI. The data developed in the two previous Design Options are subsets of the information in Table XXI and can easily be developed. In addition, other useful results can be developed. If the designer decides to change the performance requirements, a glance at the information in Tables XX and XXI will furnish him with an idea of the impact of such changes on the system cost. It is also possible to use the data in Tables XX and XXI to develop a better understanding of the basic nature of the problem. An example of this can be seen regarding the utility of the DME and VOR sensors. For a given computer, say C2, the VOR-C2 combination is shown by a Limiting Case Analysis to be more efficient than the DME-C2. If a Doppler is added to both systems, the relative efficiencies of the augmented systems switch, and the DME-Doppler-C2 is more efficient than the VOR-Doppler-C2. This is due to the fact that the VOR gives better cross-track information than the DME, while the DME provides better along-track information. When only position information is used, the cross-track disturbances affect the DME generated information more than those from the VOR. The Doppler data take care of the cross-track disturbances, thus, letting the DME provide good along-track data. Another way of stating this effect is that the DME and the Doppler tend to complement each other better than the VOR and the Doppler.

TABLE XX (Continued)

SYSTEM NO.	CONFIGURATION	COST \$ X 10 ³	PERFORMANCE (nm)	ANALYSIS	ADDITIONAL DATA
11	DME-Doppler-Decca-C2	87	< 0.1850	A.S.	
12	DME-VOR-Doppler-Decca-C2	91	< 0.1850	A.S.	
13	VOR-Doppler-C3	92	< 0.2467	A.S.	
14	DME-Doppler-C3	93	< 0.1850	A.S.	
15	DME-VOR-Doppler-C3	97	< 0.1850	A.S.	
16	Doppler-Decca-C3	102	0.2474	O.T.	Limiting Case 0.1918 nm
17	VOR-Doppler-Decca-C3	106	< 0.2467	A.S.	
18	DME-Doppler-Decca-C3	107	< 0.1850	A.S.	
19	DME-VOR-Doppler-Decca-C3	111	< 0.1850	A.S.	

TABLE XXI (Continued)

SYSTEM NO.	CONFIGURATION	COST \$ X 10 ³	PERFORMANCE (nm)	ANALYSIS	ADDITIONAL DATA
13	DME-Doppler-C1	53	0.2509	O.T.	Limiting case 0.1959 nm
14	Decca-C2	54	0.8616	L.C.	This also optimum value
15	DME-VOR-Doppler-C1	57	0.2505	O.T.	Limiting case 0.1761 nm
16	VOR-Decca-C2	58	0.3068	L.C.	
17	DME-Decca-C2	59	0.3360	L.C.	
18	Doppler-Decca-C1	62	0.3763	L.C.	
19	DME-VOR-Decca-C2	63	0.2827	O.T.	Limiting case 0.2349 nm
20	VOR-C3	64	0.2585	O.T.	Limiting case 0.2499 nm
21	DME-C3	65	0.3176	L.C.	
22	VOR-Doppler-Decca-C1	66	0.3377	O.T.	Limiting case 0.2402 nm
23	DME-Doppler-Decca-C1	67	0.2506	O.T.	Limiting case 0.1941 nm
24	Doppler-C2	68	1.467	L.C.	This also optimal value

TABLE XXI (Continued)

SYSTEM NO.	CONFIGURATION	COST \$ X 10 ³	PERFORMANCE (nm)	ANALYSIS	ADDITIONAL DATA
37	Doppler-C3	88	1.441	L.C.	This also optimal value
38	DME-VOR-Doppler-Decca-C2	91	< 0.1850	A.S.	
39	VOR-Doppler-C3	92	< 0.2467	A.S.	
40	DME-Doppler-C3	93	< 0.1850	A.S.	
41	DME-VOR-Doppler-Ce	97	< 0.1850	A.S.	
42	Doppler-Decca-C3	102	0.2474	O.T.	Limiting case 0.1918
43	VOR-Doppler-Decca-C3	106	< 0.2467	A.S.	
44	DME-Doppler-Decca-C3	107	< 0.1850	A.S.	
45	DME-VOR-Doppler-DECCA-C3	111	< 0.1850	A.S.	

Chapter 7

SUMMARY AND RECOMMENDATIONS

7.1 SUMMARY

The Design Procedure developed in this report represents the first application of automatic computation to the design of Multi-Sensor Navigation Systems. In the process of the formulation of the Design Procedure, several important decisions were required. After a general examination of the total design process, it was decided that the portion of the process which involves the iterative evaluation of systems was best suited for application of automatic computation techniques. Also, the system accuracy and cost were selected as the measures of system performance (other factors such as maintainability and reliability can be introduced by the system designer in his selection from the results of this Design Procedure). The important design parameters affecting navigation system accuracy and cost were identified and modeled mathematically. This work involved the technique of linearization of the nonlinear vehicle dynamics and measurements about a nominal trajectory to obtain linearized system dynamics, as well as measurement errors and geometric sensitivity of the navigation sensors. The model of the sensors includes sampling rate limiting which recognizes the fact that the rate at which the sensor can be sampled is limited by the physical availability of information or by computer sampling limitations. The onboard computer was also modeled. The computer's finite processing capability was modeled as an instantaneous constraint acting throughout the flight. The computer model also recognizes the different computer loadings of the various navigation measurements. These models are combined in a mathematical framework in which the measurements are processed using a Least-Squares Estimation routine.

Once the basic model of the navigation system was formulated, a technique was required to determine the accuracy limitation of any choice of navigation system configuration; i.e., any choice of a set of onboard sensors plus an onboard computer. A numerical optimization procedure was developed that iteratively adjusts the times at which the sensors are turned on and off. This procedure makes use of a formulation that models the measurement process in terms of continuous measurement rates. This formulation of the measurement process is useful in that it allows the sensors sampling rates and the computer processing constraints to assume their natural form. This greatly reduces the complexity involved in determining the optimal switching histories.

7.2 RECOMMENDATIONS

To increase the general utility of the Design procedure, research is recommended directed toward improving the efficiency and flexibility of the Design Procedure and toward broadening the class of navigation systems to which the procedure applies.

7.2.1 Procedure Efficiency and Flexibility

The major measure of the efficiency of the Design Procedure is the time required to determine the outputs of the design options and auxiliary data. The portion of the Design Procedure that uses the most time is the Optimization Technique. Two methods exist for reducing the time required to arrive at an optimal measurement schedule. An obvious method for reducing the time to generate an optimization is to run the program on a faster computer. For example, if an IBM 360 were used instead of the SDS 9300, it is estimated the time to perform an optimization could be reduced by a factor of four. A second method which gives a reduced optimization time is the application of hybrid computational techniques (refs. 27, 28) to the problem. A properly used hybrid computer takes advantage of the strong points of both the analog and digital computation processes. The analog computer is very efficient at integrating differential equations and carrying out parallel operations. The digital computer provides very accurate calculation. For the present problem, the same general optimization procedure would be recommended as presented in Chapter 4. This involves iteration on only a few switchpoints at a time. The integration of the covariance equation, however, would be done rapidly on the analog computer. This would greatly reduce the time required to perform one iteration, since this iteration, when done digitally, uses about two-thirds of the time required to perform one iteration. The lower accuracy of the analog integration as compared with that performed on the digital computer is not a problem for at least the initial iterations. The time history of the covariance matrix is sampled and transmitted to the digital machine for storage. The backward integration of the costate equation, the calculation of the switching curves, and the application of the optimal switching logic are done in the digital computer, due to the large dynamic range and required accuracy. If, at some point, the analog integration were not accurate enough, the process could be then switched over to full digital solution for the final few iterations. The time savings resulting from the use of such a hybrid procedure could be substantial.

An optimization procedure required to solve this problem is more complicated than that given in Chapter 4 for two reasons. First, the existence of optimal singular measurement sampling rates; i.e., sampling histories which do not use all the computer capacity, must be considered. Although techniques (ref. 10) exist that determine these singular controls, the logic required is complex. The second complication arises due to the fact that the terminal condition is a constraint rather than part of the cost function. Therefore, there is no specified terminal value of Λ , the costate matrix. An iterative loop must be added which determines the value of $\Lambda(T)$ which gives $\text{tr}[AP(T)] = \hat{P}$.

A second extension of the problem is the inclusion of internal constraints on the estimation errors. These constraints could be at a finite number of discrete points along the trajectory or for continuous segments of the trajectory. In the case of constraints imposed at discrete points in the flight, one method of solution would be to determine the optimal measurement schedule between two way-points using the technique of Chapter 4. Although this would not necessarily give the optimal total flight measurement schedule, it would be a close approximation. If the optimal were required or if continuous constraints were imposed, then a new optimization procedure would be required. Although work has been done on this type problem (ref. 6), the development of such an optimization procedure would require original research in both the theoretical and numerical aspects of the problem.

or

$$Z(t) = \phi(t, T) Z(T) \phi^T(t, T) \quad (A.6)$$

where $\phi(t, T)$ satisfies

$$\dot{\phi} = \left(F + P^{-1}Q \right) \phi \text{ with } \phi(T, T) = I \quad (A.7)$$

Applying Theorem 2 to Eq. (A.6) indicates $Z(t)$ is positive semidefinite.

A final application of Theorem 2 to HZH^T gives $-SW = R^{-1}HP\Lambda PH^T$ as positive semidefinite. Applying Theorem 1 to $-SW$ gives

$$-(SW)_{ii} \geq 0 \quad i = 1, \dots, m \quad (A.8)$$

or

$$SW_{ii} \leq 0 \quad i = 1, \dots, m$$

Q.E.D.

Theorem 4: For the estimation error covariance matrix $P(t)$ which satisfies

$$\dot{P} = FP + PF^T - PH^TNR^{-1}HP + Q \quad (A.9)$$

with $P(t_0) = P_0$ and performance index $J = \text{tr}[AP(T)]$, the following is true. For A a positive semidefinite matrix and $\delta P_0 = 0$ then $\delta N \geq 0$ implies $\delta J \leq 0$.

Proof: Taking the first variation of Eq. (A.9) assuming no variation in F , H , R or Q

$$\begin{aligned} \delta \dot{P} = & \left(F - PH^TNR^{-1}H \right) + \delta P \left(F^T - H^TNR^{-1}HP \right) \\ & - PH^T \delta NR^{-1}HP \end{aligned} \quad (A.10)$$

Defining the projected variation in the covariance matrix $\overline{\delta P} = \phi(t, T) \delta P(t) \phi^T(t, T)$ an expression for the value of $\overline{\delta P}(T)$ is derived in Appendix F as

APPENDIX B

NAVIGATION IN A BENIGN ENVIRONMENT

An interesting special case of the scheduling of navigation measurements is navigation in a benign environment; that is when there is no external driving noise on the system. This problem arises in the navigation of a vehicle in free space when the disturbing effects of solar pressure, gravitational perturbations, or for near earth trajectories, aerodynamic drag are small enough to be ignored.

In addition to being physically meaningful, this special case has several interesting mathematical properties. For $Q = 0$, Eq. (4.2) governing the propagation of the estimation error covariance matrix, $P(t)$, simplifies to

$$\dot{P} = FP + PF^T - PH^TNR^{-1}HP \quad (B.1)$$

This equation is still a non-linear differential equation, but it is now possible to derive an equivalent linear differential equation in the matrix S where $S = P^{-1}$. Since P is a measure of the uncertainty in the estimation of state variables, S corresponds to the knowledge of the state variables. Using this transformation in Eq. (B.1), it can be shown that

$$\dot{S} = -F^TS - SF + H^TNR^{-1}H \quad (B.2)$$

For this equation, the information rate $\dot{i} = H^TNR^{-1}H$ acts as a driving function which tends to increase the knowledge of the state. Also for a stable dynamic system where F has negative characteristic roots, the natural mode of the system is to diverge toward infinite knowledge (the uncertainties decay toward zero).

The necessary condition for optimal $N(t)$ can be determined as in Section 4.2.2 (Necessary Conditions, by applying the Maximum Principle to the system Hamiltonian. In terms of S and its co-state matrix ϕ , \mathcal{H} is

$$\mathcal{H} = \text{tr} \left\{ \psi \left[-F^TS - SF + H^TNR^{-1}H \right] \right\}$$

or

$$\mathcal{H} = \text{tr} \left\{ \left(R^{-1}H\psi H^T \right) N - \psi \left(F^TS + SF \right) \right\} \quad (B.3)$$

APPENDIX C

CHARACTERISTICS OF DIGITAL PROGRAM

The iterative optimization procedure of Chapter 4 was programmed on a Scientific Data System 9300 digital computer. The characteristics of the SDS 9300 are given in Table (C.1). Because of the short word length, the computer is hard wired so that double precision operations and storage are used automatically throughout the program. With this arrangement, the computations had eleven decimal digits of accuracy, but only 16 K words of memory. The program was written in *FORTAN IV*. It required a deck of approximately 1000 cards and 10 K words of storage. In addition some 16 K words of memory were required for variable storage, most of which was required to store the time history of the 4 x 4 covariance matrix P.

The number of iterations required to find an optimal measurement schedule requires approximately 2 to 4 times the number of switch times in the optimal measurement history. Each iteration requires 300-400 times steps to integrate from $t = 0$ to $t = 1$ hr. and this takes 4 to 5 minutes in real-time.

TABLE (C-1)

Double Precision Characteristics of SDS 9300
Digital Computer

Wordlength	48 bits
Add Time	5.25 μ sec.
Multiply Time	8.75 μ sec.
Cycle Time	1.75 μ sec.
Memory	16,000 words

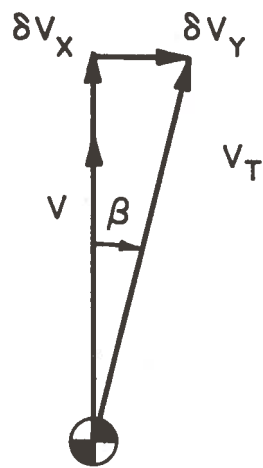
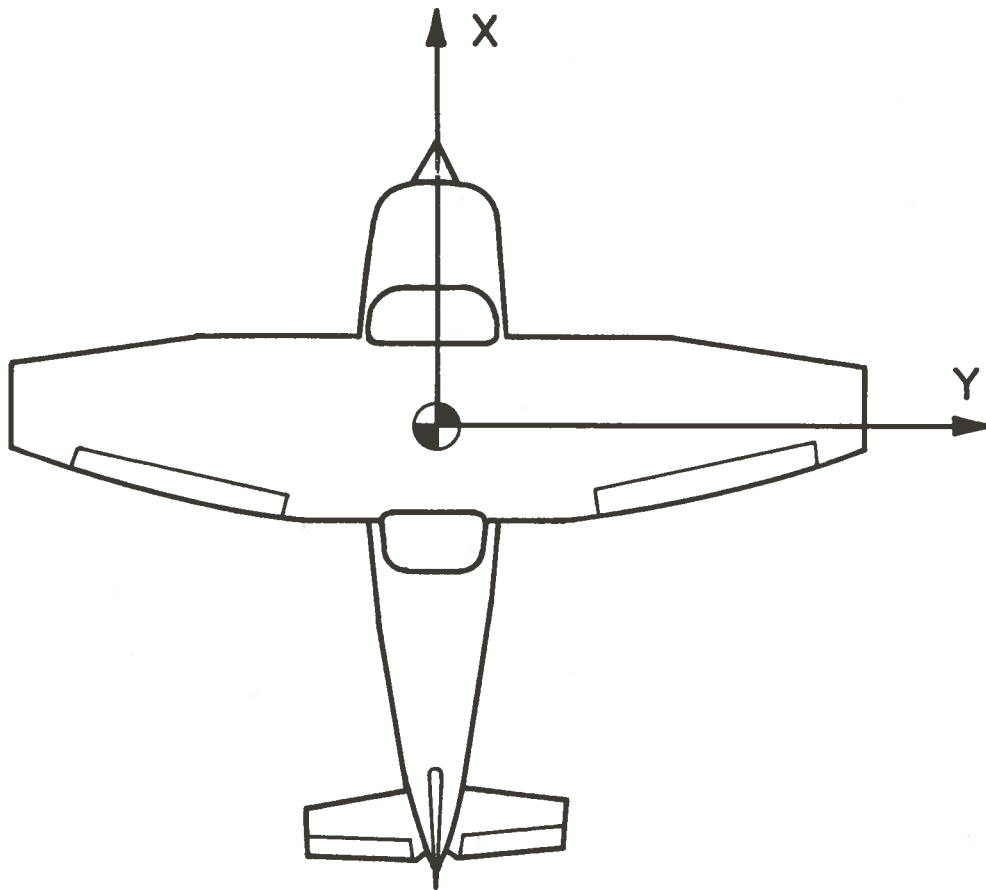


Figure D-1.- Vehicle geometry

$$\sigma_{\delta a_y}^2 = \left[\frac{\frac{1}{2} \rho V A_S}{m} C_{Y\beta} \right]^2 \sigma_{\delta V_y}^2 \quad (D.6)$$

D.3 EQUIVALENT WHITE NOISE ACCELERATION PERTURBATION

The white noise power spectral density of the longitudinal (Q_{33}) and the lateral (Q_{44}) gust generated accelerations can be written (ref. 6)

$$Q_{33} = 2 \sigma_{\delta a_x}^2 \tau_x \quad (D.7)$$

and

$$Q_{44} = 2 \sigma_{\delta a_y}^2 \tau_y \quad (D.8)$$

where τ_x and τ_y are the characteristic times for the x and y gusts. Assuming the gust field is isotropic, then

$$\sigma_{\delta V_x}^2 = \sigma_{\delta V_y}^2 = \sigma_V^2 \quad (D.9)$$

and

$$\tau_x = \tau_y = \tau \quad (D.10)$$

and finally

$$Q_{33} = \frac{2D^2}{V^2 m^2} \tau \sigma_V^2 \quad (D.11)$$

$$Q_{44} = \frac{1}{8} \left[\frac{\rho V A_S}{m} C_{Y\beta} \right]^2 \tau \sigma_V^2 \quad (D.12)$$

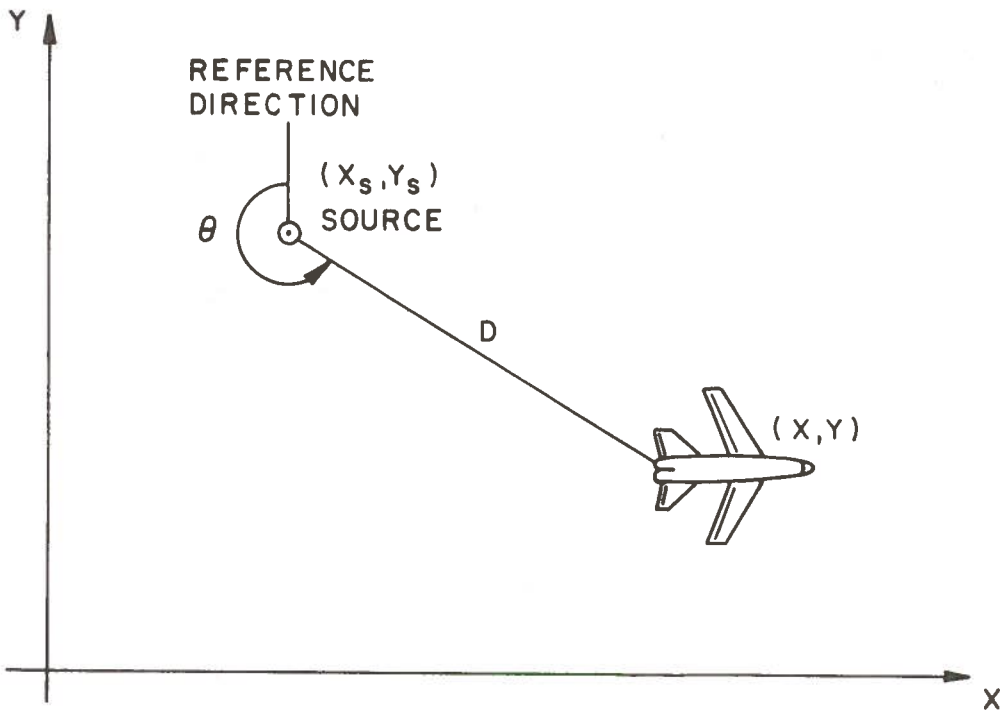


Figure E-1.- Geometry for VOR and DME navigation aids

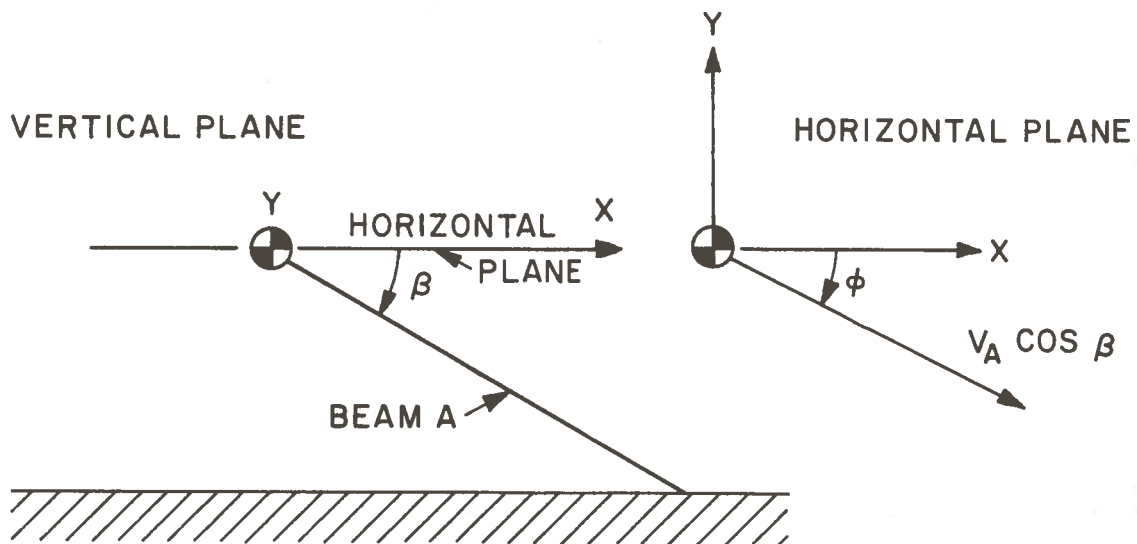


Figure E-2.- Doppler radar geometry

APPENDIX F

PERFORMANCE INDEX SENSITIVITY FOR
VARIATIONS IN CONTROL HISTORY

The equation satisfied by the estimation error covariance matrix $P(t)$ is

$$\dot{P} = FP + PF^T - PH^TNR^{-1}HP + Q \quad (F.1)$$

with $P(0) = P_0$

Taking the first variation of Eq. (F.1) considering F , H , R and Q fixed gives

$$\begin{aligned} \dot{\delta P} = & F\delta P + \delta PF^T - PH^TNR^{-1}H\delta P - \delta PH^TNR^{-1}HP \\ & - PH^T\delta NR^{-1}HP \end{aligned}$$

or

$$\begin{aligned} \dot{\delta P} = & (F - PH^TNR^{-1}H)\delta P + \delta P(F^T - H^TNR^{-1}HP) \\ & - PH^T\delta NR^{-1}HP \end{aligned} \quad (F.2)$$

Define the projected variation in the covariance matrix $\overline{\delta P}$ as

$$\overline{\delta P} = \phi \delta P \phi^T \quad (F.3)$$

where ϕ is the transition matrix defined by

$$\dot{\phi} = -\phi \tilde{F} \quad (F.4)$$

with $\phi(T, T) = I$ and $\tilde{F} = F - PH^TNR^{-1}H$

Using Eqs. (F.2, F.3, and F.4) the differential equation $\overline{\delta P}$ satisfies is

$$\dot{\overline{\delta P}} = -\phi PH^T\delta NR^{-1}HP \phi^T \quad (F.5)$$

APPENDIX G

DESIGN PROCEDURE SYSTEM LISTING AND ANALYSIS SUMMARY

A list of the 45 candidate systems ordered according to cost is given in Table G.1. Also included in this table are the results of the analyses. The type of analysis used is indicated by the abbreviations L.C. - Limiting Case, O.T. - Optimization Technique and A.S. - Augmented System. When the Augmented System concept is used, the performance is only an upper bound. This is indicated by the use of the less than inequality sign (<).

TABLE G.1 (Continued)

SYSTEM NO.	CONFIGURATION	COST \$ X 10 ³	PERFORMANCE (nm)	ANALYSIS	ADDITIONAL DATA
13	DME-Doppler-C1	53	0.2509	O.T.	Limiting case 0.1959 nm
14	Decca-C2	54	0.8616	L.C.	This also optimum value
15	DME-VOR-Doppler-C1	57	0.2505	O.T.	Limiting case 0.1761 nm
16	VOR-Decca-C2	58	0.3068	L.C.	
17	DME-Decca-C2	59	0.3360	L.C.	
18	Doppler-Decca-C1	62	0.3763	L.C.	
19	DME-VOR-Decca-C2	63	0.2827	O.T.	Limiting case 0.2349 nm
20	VOR-C3	64	0.2585	O.T.	Limiting case 0.2499 nm
21	DME-C3	65	0.3176	L.C.	
22	VOR-Doppler-Decca-C1	66	0.3377	O.T.	Limiting case 0.2402 nm
23	DEM-Doppler-Decca-C1	67	0.2506	O.T.	Limiting case 0.1941 nm
24	Doppler-C2	68	1.467	L.C.	This also optimal value

TABLE G.1 (Continued)

SYSTEM NO.	CONFIGURATION	COST \$ X 10 ³	PERFORMANCE (nm)	ANALYSIS	ADDITIONAL DATA
38	DME-VOR-Doppler-Decca-C2	91	< 0.1850	A.S.	
39	VOR-Doppler-C3	92	< 0.2467	A.S.	
40	DME-Doppler-C3	93	< 0.1850	A.S.	
41	DME-VOR-Doppler-C3	97	< 0.1850	A.S.	
42	Doppler-Decca-C3	102	0.2474	O.T.	Limiting case 0.1918 nm
43	VOR-Doppler-Decca-C3	106	< 0.2467	A.S.	
44	DME-Doppler-Decca-C3	107	< 0.1850	A.S.	
45	DME-VOR-Doppler-Decca-C3	111	< 0.1850	A.S.	

14. DeGroot, L. E. and Polhemus, W. L.: Navigation Management: The Integration of Multiple Sensor Systems. Navigation, vol. 14, no. 3, 1967-68.
15. Dodington, S. H.: Ground-Based Radio Aids to Navigation. Navigation, vol. 14, no. 4, 1967-68.
16. Blakelock, J. H.: Automatic Control of Aircraft and Missiles. New York, Wiley and Sons, Inc., 1965.
17. Babister, A. W.: Aircraft Stability and Control. New York, MacMillan Company, 1961.
18. Etkin, B.: Dynamics of Flight. New York, Wiley and Sons, Inc., 1959.
19. Taylor, J. W. R.: Jane's All the World's Aircraft. New York, McGraw-Hill Co., 1967-68.
20. Press, H., Medows, M., Hadlock, I.: A Re-Evaluation of Data on Atmospheric Turbulence and Airplane Gust Loads for Application in Spectral Calculations. NASA report 1272, 1956.
21. Cramer, H.: The Elements of Probability Theory. New York, Wiley & Sons, 1955.
22. Hildebrand, F. B.: Methods of Applied Mathematics. Prentice-Hall, Inc., N. J., 1952.
23. Gaines, H. T., Hilal, A. K., and Kell, R. J.: Computer Recommendations for an Automatic Approach and Landing System for V/STOL Aircraft. Vol. 1, NASA/ERC Contractors Report, Contract Number NAS 12-615, June 1968.
24. Ergin, E. I.: Advanced SST Guidance and Navigation System Requirements Study Final Report. Vol. 1-3, NASA/ERC Contractors Report, Contract Number NAS 12-510, April 1967.
25. Aoki, M. and Ki, M. T.: Optimal Discrete-Time Control System with Cost for Observation. IEEE Trans. on Auto Control, vol. AC-14, no. 2, April 1969.
26. Kushner, H. J.: On the Optimum Timing of Observations for Linear Control Systems with Unknown Initial State. IEEE Trans. Automatic Control, vol. AC-9, April 1964.
27. Bekey, G. A. and Karplus, W. J.: Hybrid Computation. Wiley and Sons, New York, 1968.